CATÓLICA
ESCOLA SUPERIOR DE BIOTECNOLOGIA
PORTO

DESIGN AND ASSEMBLY OF MICROFLUIDIC PAPER-BASED ANALYTICAL DEVICES (μPADs) FOR THE QUANTIFICATION OF NITRITE AND NITRATE IN SALIVA

by
Francisca Teixeira Soares da Mota Ferreira

March 2019

CATÓLICA
ESCOLA SUPERIOR DE BIOTECNOLOGIA
PORTO

DESIGN AND ASSEMBLY OF MICROFLUIDIC PAPER-BASED ANALYTICAL DEVICES (μPADs) FOR THE QUANTIFICATION OF NITRITE AND NITRATE IN SALIVA

Thesis presented to Escola Superior de Biotecnologia of the *Universidade Católica Portuguesa* to fulfill the requirements of Master of Science degree in Biomedical Engineering

by
Francisca Teixeira Soares da Mota Ferreira

Place: Escola Superior de Biotecnologia - Universidade Católica Portuguesa

Supervision: Dr. Raquel Mesquita and Prof. António Rangel

March 2019

Resumo

Nos últimos anos, investigadores, com o auxílio de novas tecnologias, têm trabalhado para o desenvolvimento de técnicas e dispositivos de diagnóstico e tratamento mais práticos e económicos.

Neste trabalho foram desenvolvidos dois dispositivos microfluídicos analíticos baseados em papel (μPADs) para a determinação dos aniões nitrito e nitrato em amostras de saliva humana, para auxílio no diagnóstico de doenças associadas à sua presença. Para desenvolver estes μPADs foram realizados vários estudos de desenho e construção, incluindo um teste de interferências e estudos de estabilidade.

A estrutura final do μPAD para a determinação de anião nitrito consistiu em duas camadas de discos de papel de filtro com 9.5 mm de diâmetro numa bolsa de plastificação, em que a última camada continha 5 μL de reagente de Griess. Este μPAD permitiu a determinação de nitrito num intervalo de 5 – 220 μM, cujos limites de deteção e quantificação foram 0.05 μM e 0.17 μM, respetivamente. A estrutura final do μPAD para a determinação de anião nitrato consistiu em três camadas de papel de filtro numa bolsa de plastificação, em que a primeira camada continha zinco em pó e a última camada 10 μL de reagente de Griess. Este μPAD permitiu a determinação de anião nitrato num intervalo de 0.2 – 1.2 mM, cujos limites de deteção e quantificação foram 0.08 mM e 0.27 mM, respetivamente.

Ambos os μPADs se mostraram estáveis quando armazenados em vácuo (durante pelo menos 7 dias no caso do μPAD de nitrito, e durante no máximo 3 dias no caso do μPAD de nitrato) e, após colocação da amostra, os μPADs de nitrito e nitrato poderiam ser digitalizados até 4 e 2 horas depois, respetivamente.

Por último, para validar este método, os resultados obtidos com o μPAD de nitrito foram comparados com os correspondentes aos obtidos pelo método colorimétrico de referência, e não foram encontradas diferenças estatisticamente significativas entre os dois métodos. Logo, foi possível concluir que os μPADs desenvolvidos demonstraram possuir propriedades promissoras para a determinação de NO_X em amostras de saliva, principalmente porque são dispositivos sensíveis, portáteis, simples e económicos, que custam menos de 50 cêntimos cada.

Palavras-chave: μPAD; nitrito; nitrato; saliva; reação de Griess

Abstract

In the last few years, researchers, with the help of new and advanced technologies, have been working towards the development of more practical and more affordable, diagnostic and treatment devices and techniques.

In this work, two different Microfluidic Paper-based Analytical Devices (μPADs) were developed for the determination of nitrite and nitrate in human saliva samples to aid in the diagnosis of some diseases and health conditions associated with these ions. To develop these nitrite and nitrate μPADs, several studies were performed to optimize the design and construction, including an interference assessment and stability studies.

The final structure of developed μPAD for the nitrite determination consisted of two layers of 9.5 mm diameter filter paper disks within a plastic laminating pouch, in which the bottom layer contained 5 μL of Griess reagent. This μPAD allowed a nitrite determination in a range of 5 - 220 μM with limits of detection and quantification of 0.05 μM and 0.17 μM, respectively. The nitrate μPAD final structure consisted of three layers of filter paper, also within a plastic laminating pouch, in which the top layer contained the zinc powder and the bottom layer contained 10 μL of Griess reagent. This μPAD allowed a nitrate determination in the range 0.2 – 1.2 mM with limits of detection and quantification of 0.08 mM and 0.27 mM, respectively.

Both of the μPADs were stable when stored in vacuum (the nitrite μPAD for at least 7 days and the nitrate μPAD for a maximum of 3 days) and, after the sample placement, the nitrite and nitrate μPADs could be scanned within the first 4 and 2 hours, respectively.

Finally, to validate this method, nitrite μPAD measurements were compared with the ones obtained from the standard colorimetric method and there were no statistically significant differences between these two methods. So, it was possible to conclude that the developed μPADs exhibited promising properties for NO_X determinations in saliva samples, especially because they are sensitive, portable, simple and affordable devices that cost less than 50 cents each.

Keywords: μPAD; nitrite; nitrate; saliva; Griess reaction

Acknowledgments

First, I would like to thank my supervisors, Professor Doctor António Rangel and Doctor Raquel Mesquita, for all the help, guidance and knowledge provided through the entire duration of this thesis, both in the laboratory and during the thesis writing. For the opportunities in presenting this work in conferences, which allowed me to grow both personally and professionally, I am deeply thankful. Without them, the development of this thesis would not be possible.

I would also like to thank my laboratory co-workers, which provided daily support and help through this entire journey.

To my family and friends, I would like to thank them for supporting me through all the ups and downs, celebrating with me in my achievements and not let me lose my mind in the tough times.

Last but not least, I would like to thank the Escola Superior de Biotecnologia of Universidade Católica Portuguesa, for providing the space and all the materials used in the development of this thesis.

Contents

1. Introduction

According to the World Health Organization, “more people can access essential health services today than ever before, but at least half of the world’s population still go without” the basic health care (1).

With the advances in technologies, new innovative techniques have been developed. However, it still exists a lack of practical and affordable devices that are capable of performing diagnosis and treatments on location, whether it be in a medical institution, in the patients’ homes or in the most secluded areas. The population living in the less developed countries commonly encounter obstacles in accessing the basic health care, not only because of economic or geographical difficulties but also lack of skilled professionals to performed the tests. (2,3).

That is why in the last few years, researchers have been working towards the development of new diagnostic and treatment devices and techniques that follow the seven “ASSURED” guidelines provided by the World Health Organization for the selection of diagnosis tests, namely being Affordable, Sensitive, Specific, User-friendly, Rapid and Robust, Equipment-free, and Deliverable to end-users (4,5).

1.1. Microfluidic Paper-based Analytical Devices

In 2007, Martinez A. *et al.* introduced for the first time the concept of microfluidic paper-based analytical device, or μPAD, as a “platform for inexpensive, low-volume, portable bioassays”(6,7). After that, the research on this type of devices increased exponentially in areas as healthcare, environmental, food and water (8). Even though there are currently several different types of μPADs, the principle in which all of them are based consists in the presence of two different areas: a hydrophilic area provided by the paper where a reaction (usually colorimetric) occurs, and a hydrophobic area that delimits this reaction zone (4,8).

Although this concept is recent, the use of paper for analytical detection reports back to the use of litmus paper as an acid-base indicator by Boyle in the XVII century (8). The main characteristics that make paper an appealing tool are the low cost and the high availability. However, there are other advantages such as the fact that paper is lightweight, available in several thicknesses and porosities, easy to store and transport and compatible with biological samples (because of its cellulose matrix) (9).

As it was mentioned before, there are currently μPADs that use detection methods such as luminescence, electrochemical and photoelectrochemical detection, but the most commonly

used is the colorimetric detection, mainly because it has a simpler and easier way of interpreting the results. With colorimetric reactions, the results can be easily interpreted visually or captured with digital cameras, mobile phones or portable scanners (6,8). Then the colour intensities produced in the colorimetric test can be determined from the digital images by using image processing programs such as ImageJ and converted in absorbance values using the Beer-Lambert law:

$$A = \log_{10}(I_0/I_S)$$

where A is the absorbance value, I_S is the mean measured intensity (of the image pixels) of the standard or sample, and I_0 is the mean measured intensity (of the image pixels) of the blank (8,10).

However, a disadvantage of these colorimetric detection methods is the high variability, caused for example by a non-uniform distribution of the coloured product in the paper. This problem can be reduced by using more replicas and excluding outliers, if necessary (8).

To build a μPAD, first it is necessary to define the hydrophobic and hydrophilic areas. This can be achieved either by cutting the paper or creating hydrophobic boundaries within the paper. The latter option can still be divided in a direct approach, where a hydrophobic liquid material is printed in the paper, and an indirect approach that involves more complicated procedures to create these hydrophobic zones (Figure 1).

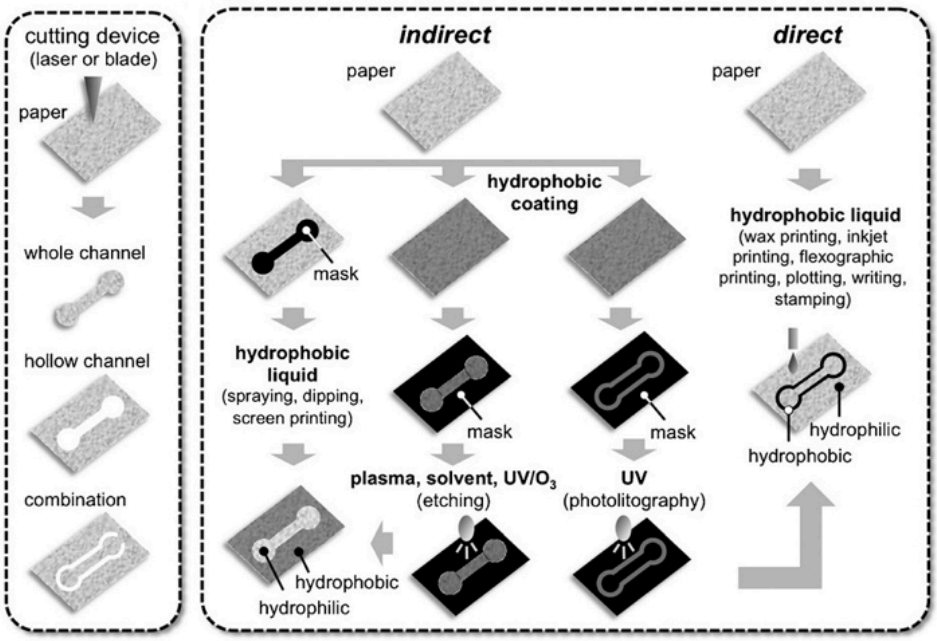

Figure 1 - Schematics of the approaches in creating the hydrophilic and hydrophobic areas (6).

Even though there are several materials that can be used to pattern these areas, like polydimethylsiloxane (PDMS), indelible ink and polystyrene, the most commonly used to design μPADs is wax, because it is a simple and relatively quick method (Figure 2) that is compatible with most μPAD applications, and it is not a risk to the environment since it can be disposed by burning (4,6). Nevertheless, this type of printing method requires expensive wax and an extra step of heating in the process. Also the spreading of the liquid wax when printed in the filter paper causes a decrease in the pattern's resolution.

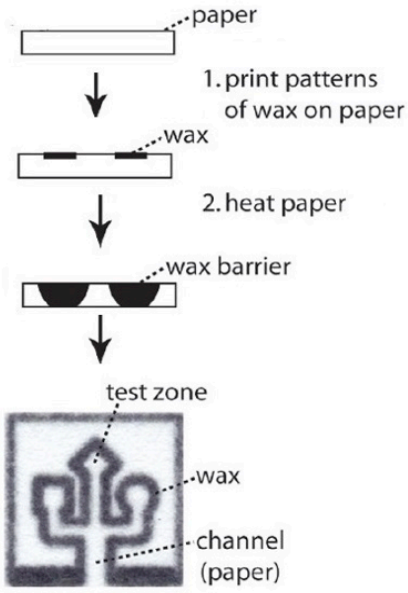

Figure 2 - Procedure of printing method with wax (6).

The first developed μPADs consisted in one layer of paper, where sample travelled horizontally in the microchannels of the paper. However, in 2008, the Whiteside group developed the first 3D μPAD, which consisted in 2D μPADs layered on top of each other and held together with the help of double-sided adhesive tape (4). These 3D μPADs have become very popular in the last few years. Because in these μPADs the sample travels both horizontally and vertically, it is possible to direct this sample into a specific path and make it react with several reagents in a specific order (4,6). Also, a higher amount of paper layers increases the sample absorption capability of the μPADs, which can be useful when the concentration expected in the determination is very low (4,6). The stack of paper layers can be held together by using adhesive tape (Figure 3A), by spraying adhesive on the paper layers or using origami, by folding the paper in to several layers (Figure 3B) (4).

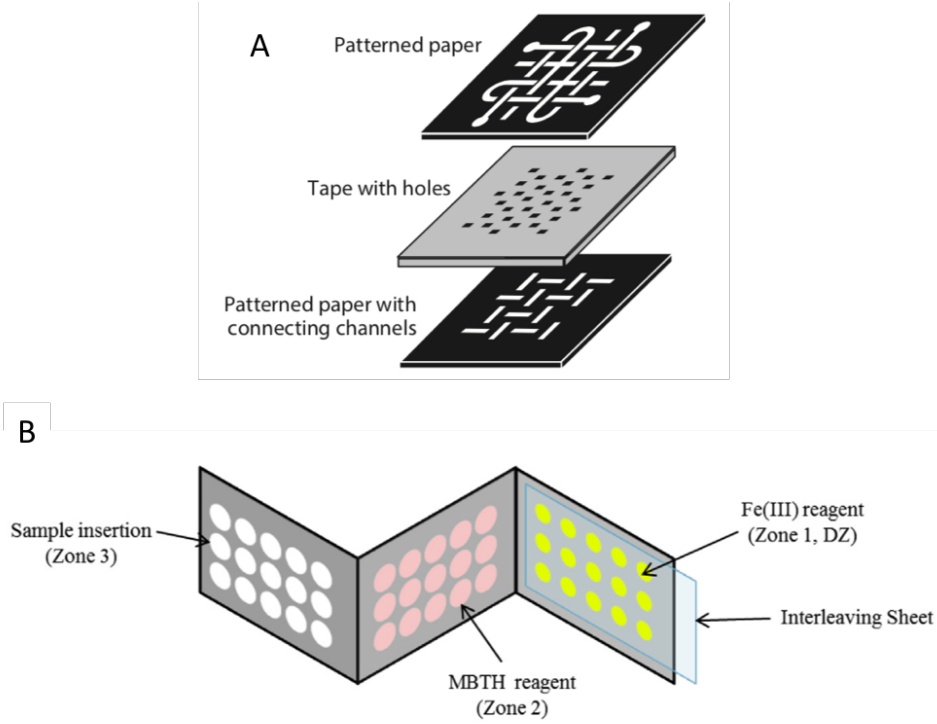

Figure 3 - (A) 3D µPAD with use of adhesive tape (4); (B) 3D µPAD constructed by origami (11).

Much of the µPADs popularity is due to their various advantages. They are simple, portable, affordable, rapid, disposable, and, after being assemble, don't require complex equipment or specialized personal to do the measurement, which makes them and interesting tool to be used in on-site analysis in locations of difficult access or with very few resources. However, very few of the developed µPADs reported so far, presented any on-field or stability studies (8). Some locations or conditions can affect the performance of these devices, therefore it is very important to test them on lab conditions, on field conditions and also their stability in different storage conditions (3,8).

1.2. Nitrite and Nitrate

Nitrite and nitrate are nitrous acid salts found everywhere, from waters, to food and even in the human body. They are composed by one nitrogen atom and two (nitrite) or three (nitrate) oxygen atoms.

Nitrite (NO_2^- ; molar mass 46.01 g/mol) has a symmetrical bent structure (Figure 4A) where both bonds have identical length and form an angle of approximately 115º. This ion has

an electron shared between the two bonds (Figure 4B) which, according to valence bond theory, makes it a resonance hybrid (12).

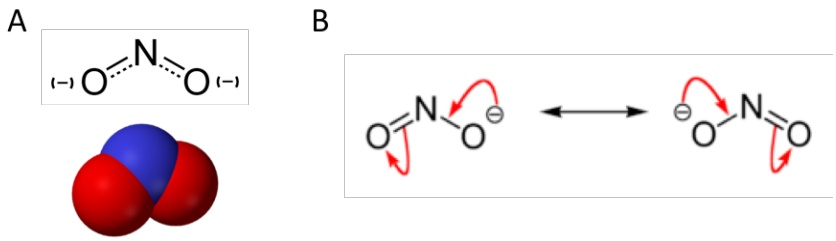

Figure 4 - (A) Nitrite ion structure; (B) Nitrite resonance hybrids. (12)

Nitrate (NO_3^- ; molar mass 62.00 g/mol), on the other hand, has a trigonal planar arrangement, carrying the formal charge of -1 between the three identical bonds (Figure 5A), which originates three resonance structures (Figure 5B) (13).

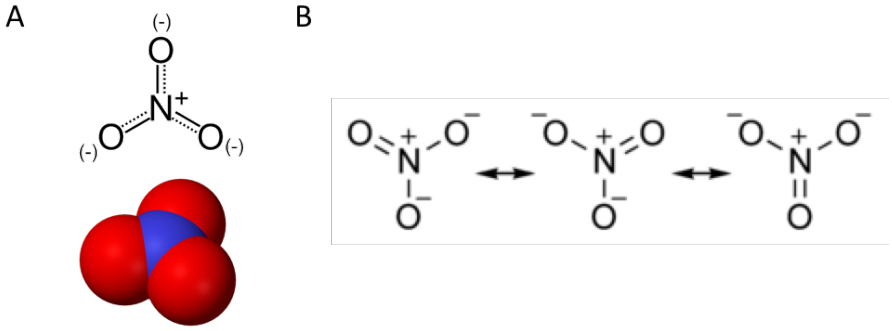

Figure 5 - (A) Nitrate ion structure; (B) Nitrate resonance hybrids (13).

The presence of these anions in the human body can be due to either an endogenous produce in the body or ingestion through food and water, but with the increase of pollution and water contamination reports, it is the last one that presents the largest threat to human health (14,15).

According to Lundberg *et al.* (2004), about 60-80% of the daily nitrate consumption (approximately 2-3 mM) comes from vegetables. Nitrate and nitrite can also be found in some foods like meat, as an additive, or even in cigarettes and car smoke (14,16). The endogenous source of nitrate in mammals is mainly the L-arginine-NO pathway, where the NO synthases use L-arginine amino acid and molecular oxygen to produce NO. This pathway, shown in Figure 6, in basal conditions, occurs primarily in the blood vessels' endothelium and neuronal tissue, but in case of infections or inflammatory reactions there is a larger production of NO

by NO synthases, released by white blood cells, which leads to higher nitrate concentrations in plasma (14). Most of NO_X is later secreted mostly in urine, but also in saliva and sweat. In fact, 25% of the nitrate present in plasma is secreted in saliva, which leads to a ten times higher concentration in saliva when compared with the plasma (14,16).

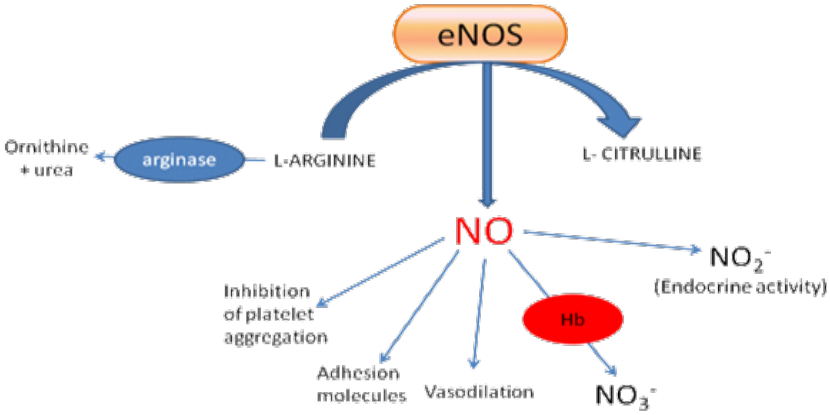

Figure 6 - Schematics of L-arginine-NO pathway.(17)

For many years these ions have been associated with cancer. Nitrite from, either direct ingestion, or the nitrate reduction by bacteria in human saliva, when it reaches the acidic environment of the stomach and combined with amine or amide forms nitrosamines and nitrosamides, which are toxic and carcinogenic, thus contributing mainly to the development of gastric cancer (15,18,19). When absorbed to the bloodstream, nitrite can react with the iron in haemoglobin, irreversibly converting it in methaemoglobin and preventing it from carrying oxygen (Figure 7). This blockage results in a blood disease called methemoglobinemia, or as is most commonly known as “blue baby” syndrome (15,16,20,21).

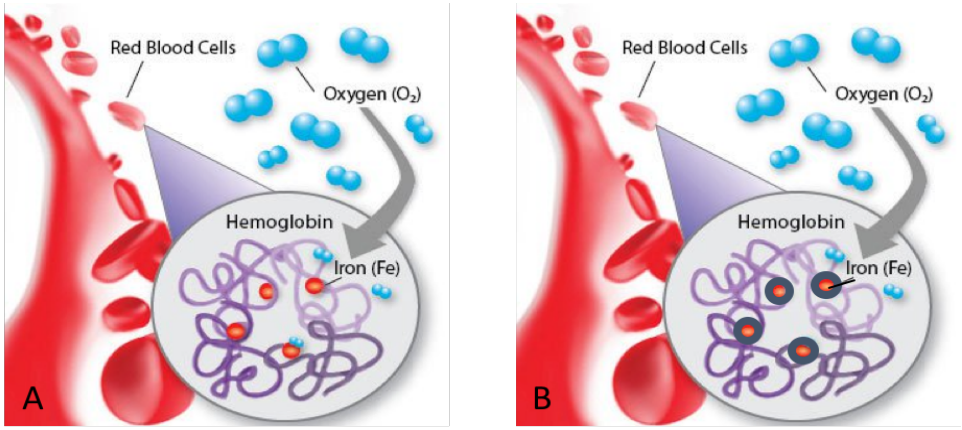

Figure 7 - (A) Normal formation of oxyhaemoglobin; (B) Formation of methaemoglobin in the presence of nitrite (Modified from (22)).

Depending on the percentage of methaemoglobin, different symptoms may be associated. But when it reaches a high percentage, it can lead to death. These symptoms can be found in Table 1.

Table 1 - Symptoms of Methemoglobinemia.

Methaemoglobin Percentage	Methemoglobinemia Symptoms
< 3%	normal healthy individuals
3 - 10%	skin discoloration (cyanosis)
10 - 20%	tachycardia, weakness, signs of tissue hypoxia
> 20%	headache, dizziness, fatigue, dyspnea, nausea
> 70%	high risk of mortality

Although less common, bladder cancer can also be a concern in cases of urinary-tract infections. Since a big amount of the nitrate is secreted in the urine, the presence of bacteria during these types of infections and lead to the nitrate conversion into nitrite, and consequently N-nitrosamine formation (14).

Even though its bad reputation, nitrate is not actually very toxic. It is only when is converted to nitrite that becomes a big concern to human health (14). Bahadoran *et al.* (2015) concluded that there was no association between nitrate exposure and thyroid cancer, but it was possible to associate nitrite exposure to thyroid cancer (risk = 1.48, 95% confidence interval = 1.09–2.02, P = 0.012) (23).

Ever since 1970s, NOx compounds have been associated with cancer and other diseases. However, recently a few studies have been reporting newly found benefits of these ions. Salivary nitrates and nitrites may not only be a defence response to oral infectious diseases like periodontal disease (24), but also present a protective effect against dental caries (25). Furthermore, the measurement of nitrite can be used to measure nitric oxide, which is involved in many metabolic procedures, like: regulation of vascular tone, inhibition of platelet aggregation, thrombosis, and inflammation, and establish a correlation with the degree of injury (15).

Nowadays, there are several methods that allow nitrite and nitrate detection and determination for a number of concentration ranges and types of samples, such as

spectrophotometric detection, electrochemical detection, chemiluminescent, chromatographic, spectrofluorimetric, capillary electrophoresis and electrochemiluminescence detection. Some of these techniques do a simultaneous and independent detection of nitrite and nitrate, being therefore classified as simultaneous methods. Others first detect nitrite and then, in order to measure nitrate, this compound is converted to nitrite. Therefore, the methods that use this last principle are known as sequential methods (15,26).

The most commonly used detection method for nitrate and nitrite determination is by far the spectrophotometry, not only because it's a relatively inexpensive method, but also because of its simple approach. It is based upon the measurement of the colour intensity in a colorimetric reaction, where colour is proportional to the concentration of the analyte. In the spectrophotometry category, the most used approach for the NOx detection and determination is the Griess reaction (15,26).

In 1879, a german chemist named Johann Peter Griess presented, for the first time, a colour reaction for the detection of NOx in saliva. According to the original Griess reaction, in an acidic environment, nitrite reacts with sulfanilic acid forming a diazonium cation which in turn reacts with **α**-naphthylamine, forming a water-soluble red-violet coloured product (15,26,27). This reaction is presented in Figure 8.

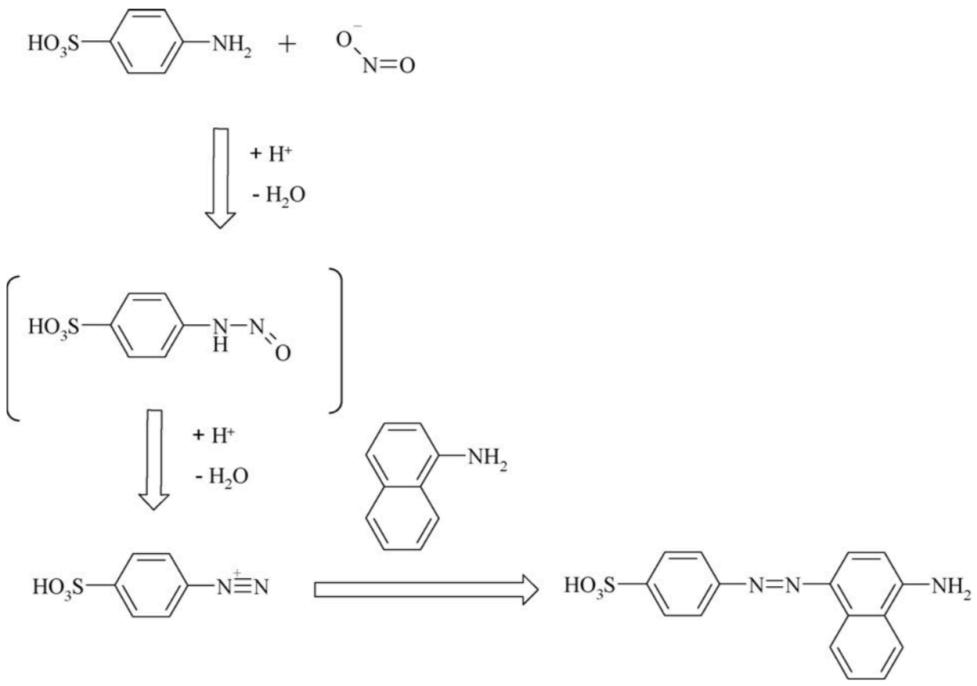

Figure 8 - Original Griess reaction reported in 1879 by Griess (27).

Because the α-naphthylamine reagent, originally used by Griess, is carcinogenic, Brantton and Marshall, in 1939, presented for the first time sulfanilamide and N1NED (N-(1-naphthyl)-ethylenediamine dihydrochloride)) as alternatives to the reagents in the first reported Griess reaction (26). This modified Griess reaction is shown in Figure 9.

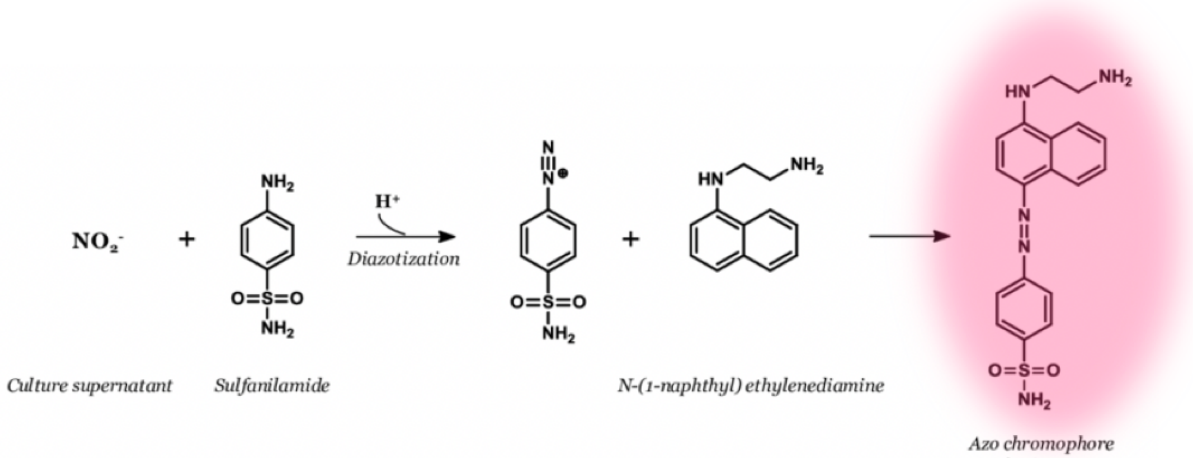

Figure 9 - Modified Griess reaction using sulfanilamide and N1NED (Modified from (28)).

To perform the nitrate determination using the Griess reaction, it is first necessary to reduce nitrate to nitrite, using reducing agents like cadmium or vanadium chloride, and only after this reduction to nitrite, the reaction with the Griess reagent occurs (27).

Although there are already numerous methods reported for the NOx determination, these methods have some limitations like requiring high volume of reagents and sample, the time of analysis, the use of complex lab equipment, the need of constant power, specialized technicians, the production of toxic waste, among others.

To perform these detection and determination techniques it is necessary to analyse a patient sample. Nowadays, the most common samples used are the biological fluids, manly blood/serum. However, this type of sample demands an invasive collection procedure and usually brings a considerable discomfort to the patient. Moreover, it requires specialized personnel, very specific storage conditions, and the invasiveness of the collection presents a risk of contamination and of spreading diseases (29,30). That is why, in the last few years there has been an increase of the interest and research in using others biological samples that could possibly replace blood analysis, such as saliva.

1.3. Saliva

Saliva is an exocrine secretion produced by the major and minor salivary glands. It is composed by 94-99% water, with several electrolytes, proteins, immunoglobulins, enzymes, mucins and nitrogenous products, and its importance in the overall human health is often overlooked (30–32). Saliva is not only essential for lubrication of the oral cavity but also protects the tissues from irritants and aids in the mastication, deglutition and speech (31). This oral fluid can additionally act as a buffer, stabilizing the pH in the oral cavity, which is usually in the range 6-7. This buffering capability blocks the colonization of certain microorganisms, since it denies the optimal conditions for their survival (31,32). Another function of saliva is maintaining the tooth integrity by playing an important part in the demineralization and remineralization processes, mainly due to the calcium, phosphate and fluoride concentrations and pH (32). Since there is a presence of several proteins in the oral fluid capable of protecting the tissues from certain microorganisms, it can be said that saliva also presents antibacterial properties (31). Although there are immunoglobulins G and M, the one most important and present in bigger quantity is immunoglobulin A, which is capable of neutralizing several types of viruses, bacteria and toxins (32). One of the crucial roles of saliva is also to initialize the digestion of starch and to solubilize dry food, which helps carry the flavours to the gustatory buds, enhancing taste (32). Since it has been observed that coagulation in a bleeding wound is faster in the oral cavity, it has been proposed in a research study that saliva also has a tissue repairing property (32).

In the last few years there has been an increase of interest in the use of saliva as a sample for substitution of blood. The collection of saliva is easier, safer and more economic when compared with blood collection (30,33,34). Saliva sampling is also a painless non-invasive procedure, with a lower risk of contamination or dispersion of contagious diseases (30,33). Moreover, due to its simplicity, saliva collection does not require specialized medical personnel, and it can be done in secluded areas and more often than the blood collection (29,30,33). As a sample, saliva has been known to contain several substances with interest for screening and diagnosis purposes and, although is preferable to be kept on ice, the samples are stable for 24 h in room temperature or for a week at 4ºC (29,30). Besides, for some groups of patients, like children, seniors or, for example, patients with blood clotting disorders, it would be easier to collect saliva, when compared with the current blood collection (30,34).

Nowadays, there are several simple ways to successfully collect saliva. The sampling can occur by passive drooling, which consists of, without any stimulation, letting the saliva

run to a plastic vial (Figure 10A), or with an assistance of materials like cotton swabs, gauzes or rolls (Figure 10B) (29,30,34).

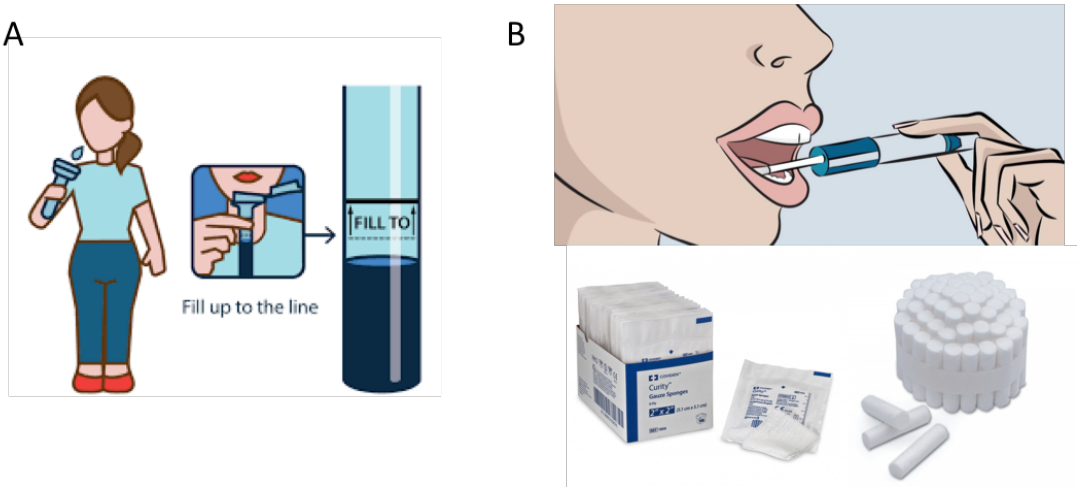

Figure 10 - (A) Plastic tube for the saliva sampling; (B) Instruments usually used to help the saliva collection (35–38).

However, because there are no perfect samples, saliva also has some disadvantages. One of the big issues of using this fluid as a sample is the lack of specific information on biomarker concentrations in saliva, mainly because it is a very recent and new approach that hasn't been extensively studied yet (29,33). Another problem can be the variations in the saliva composition that can occur accordingly to factors like age, gender, the time of the day of the sample collection and if the saliva was unstimulated or stimulated (19,32). The mean salivary nitrite and nitrate in humans, according to recent studies, was found to be between 1 - 10 mg/L and 10 - 80 mg/L, respectively (14,24,39).

1.4. Objectives

The focus of this work was to develop two new microfluidic paper-based analytical devices (µPADs) for the quantification of nitrite and nitrate anions in human saliva samples, using a new construction approach that has not been reported yet, and also using spectrophotometric detection based on the Griess reaction. The idea was for these µPADs to ultimately be capable of being used not only in healthcare facilities, but also to be taken to remote locations and aid in the diagnosis of some diseases and health conditions.

2. Materials and Methods

2.1. Reagents and Solutions

The solutions used in this work were all prepared with analytical grade chemicals and Milli-Q water, (resistivity > 18 MΩ/cm, Millipore, USA).

The standard stock solution of sodium nitrite (Merck) was prepared monthly by dissolving approximately 30 mg of the solid in 50 mL of water. A fivefold dilution of sodium nitrite stock solution was weekly made in order to prepare, also weekly, the working standards of nitrite in the range of 5 - 250 μM.

The standard stock solution of sodium nitrate (Merck) was prepared monthly by dissolving approximately 40 mg in 50 mL of water. The working nitrate standards were prepared daily from the standard stock solution in a range of 0.2 - 1.2 mM.

The Griess reagent was monthly prepared according to Mesquita R. *et al.* (40) by dissolving approximately 0.4 g of sulfanilamide (Sigma-Aldrich) in 2 mL of 5 M *ortho*-phosphoric acid and 0.04 g of N-(1-naphthyl)-ethylenediamine dihydrichloride (N1NED) (Merck) in water. These two homogenized solutions were mixed together, and the volume was completed to 20 mL. This solution was stored in a dark bottle and shielded from the light. A zinc suspension was prepared for every 4 μPADs (maximum), by mixing 1 g of zinc powder (<10 μm) (Sigma-Aldrich) in 20 mL of water.

2.2. Design and Production of the μPAD and Determination Procedure

The assembly of both of the μPADs consisted in a 75x110 mm plastic laminating pouch (Q-Connect) (hydrophobic area), previously perforated with twenty-four 4 mm holes for the sample insertion, and twenty-four sets of filter paper disks (hydrophilic area) aligned under the holes, in a 4 columns and 6 rows' distribution.

2.2.1. Nitrite μPAD

For the nitrite determination μPAD, each set of disks consisted of two circles of different paper aligned over each other as shown in Figure 11. The top layer consisted of Whatman Grade 1 filter paper and the bottom, Whatman Grade 50 filter paper. In each disk of

the bottom layer, 5 µL of the Griess reagent was added and left to dry in a 50ºC oven for 10 minutes. After the alignment of the paper disks in the laminating pouches, they passed through the laminator (Fellowes L125 - A4) thus creating a µPAD with two different zones: the hydrophobic zone provided by the plastic of the pouches, and the hydrophilic zone provided by the disks of filter paper. Then, 15 µL of sample was inserted through each of the holes made on the laminating pouches, traveling to the bottom layer, where the nitrite reacted with the Griess reagent. To prevent the evaporation of the sample and the oxidation of the Griess reagent, after the sample was fully absorbed, the holes were covered with adhesive tape.

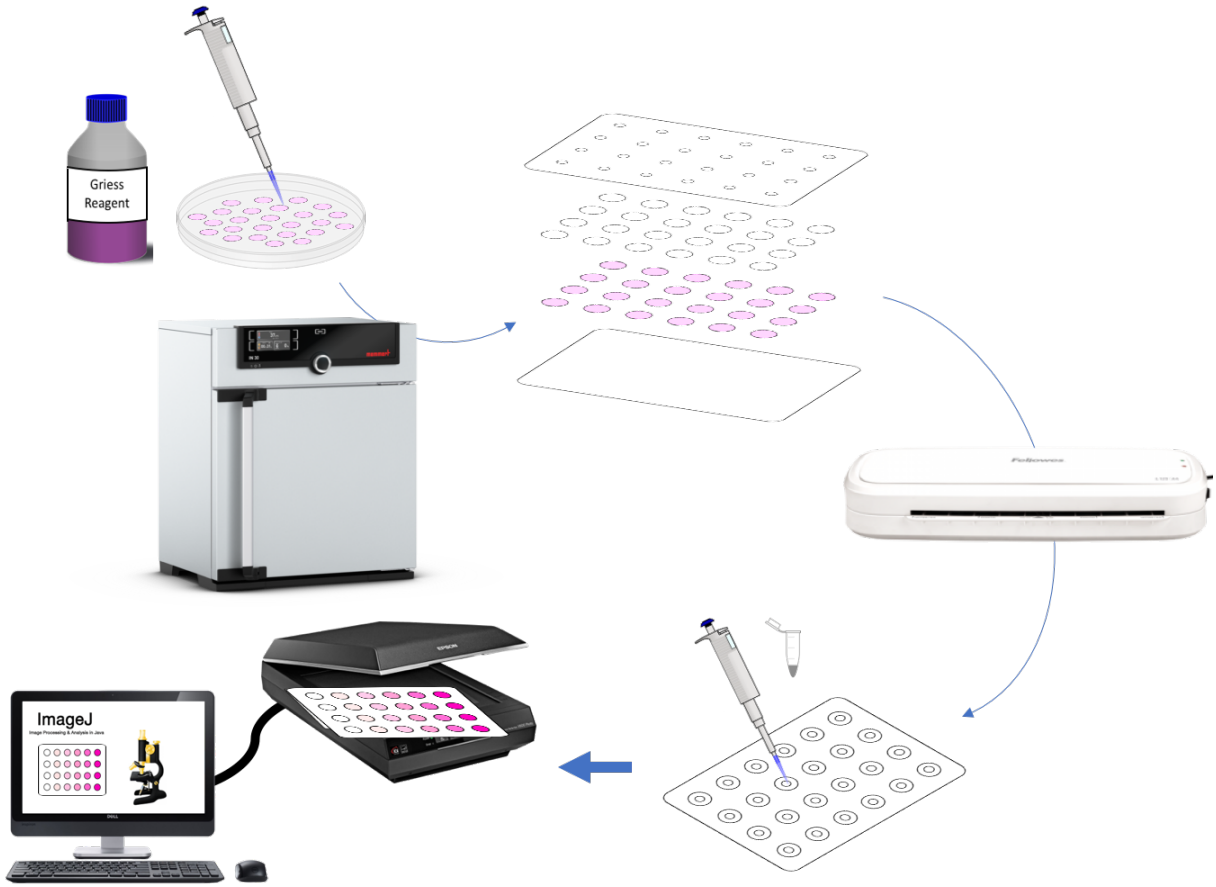

Figure 11 - Procedure followed for the assembly of the nitrite determination µPADs.

2.2.2. Nitrate µPAD

In the nitrate µPAD, each set of disks consisted of three different sizes and types of paper aligned over each other as shown in Figure 12. The first/top layer consisted of 9.5 mm diameter disks of Whatman Grade 1 filter paper, the second/middle of 1.27 cm diameter

disks of Whatman Grade 1 filter paper, and the third/bottom layer of 9.5 mm diameter disks of Whatman Grade 50 filter paper.

The disks for the first layer were embedded in a zinc suspension with manual agitation for approximately thirty seconds. Then these disks were removed and left to dry in a 50ºC oven for approximately 30 minutes. To control the amount of zinc in the paper circles, these disks were weighed before and after they were embedded in the zinc suspension. Therefore, the average amount of zinc on each circle could be calculated by determining the difference between the weights and then dividing it for the number of disks. In each circle of filter paper of the third and bottom layer, 10 µL of the Griess reagent was added and left to dry in a 50ºC oven for 10 minutes.

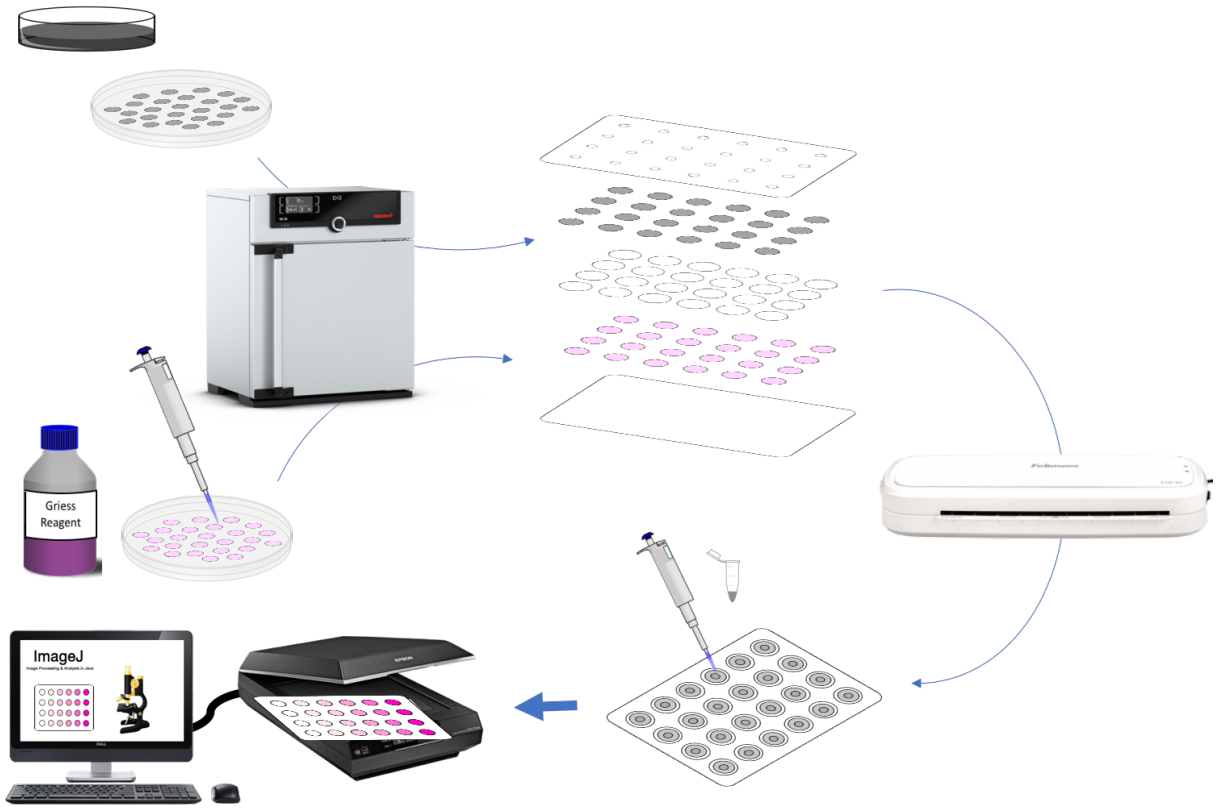

Figure 12 - Procedure followed for the assembly of the nitrate determination µPADs.

After the alignment, the laminating pouches passed through the pouch laminator (Fellowes L125 - A4). Then 25 µL of sample was inserted, traveling through the first layer where nitrate was converted to nitrite by the zinc, all the way to the bottom layer where the nitrite reacted with the Griess reagent. When the sample was completely absorbed, the holes were covered with adhesive tape.

2.2.3. Image and Data Processing

For both µPADs, the reaction product obtained had a pink colour and, the more intense the shade of pink, the higher concentration of nitrite in the sample. In order to measure the intensity of the colour, the bottom layer of the µPADs were scanned using a standard scanner (Canon LiDE 120) and the images were processed using ImageJ (National Institutes of Health, USA, https://imagej.nih.gov/ij/). In the ImageJ, these images were converted into RGB plots with "3 layers": the Red, the Green and the Blue. The colour we observe in an object is merely the result of the absorption and reflection of light in different wavelengths. If an object is observed with a particular colour, then that object absorbs light in a wavelength of a complementary colour. In Figure 13, the colour star is represented, in which colours in opposite ends of the star are complementary colours.

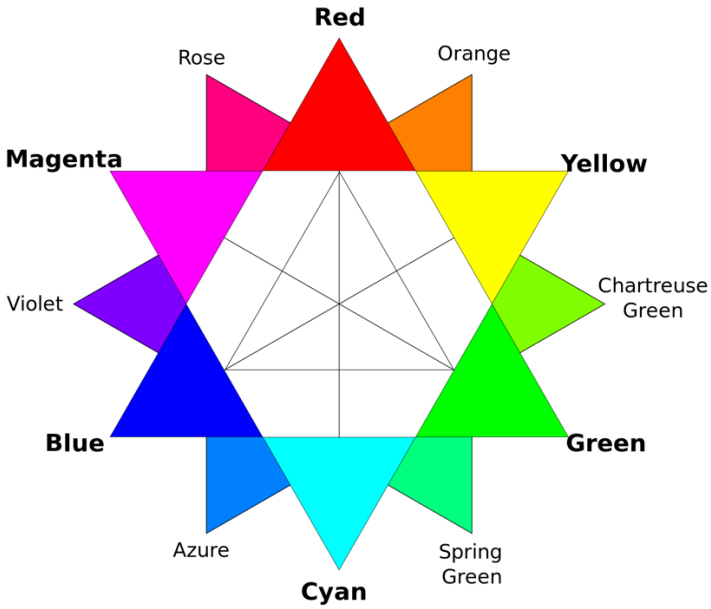

Figure 13 - RGB model colour star (41).

Since the expected coloured product of the Griess reaction is pink, then the complementary colour in which this product absorbs is the green. That is why the green "layer" of the RGB plots was used to measure the intensity of pink in the images.

For each colour disk, an option was made to do the measurements with the circular selection tool with 200x200 pixels, because it allowed better adjustment to the reagent disk area (9.5 mm diameter). As Birch and Stickle described (10), it was possible to convert the measured intensity of pink in an absorbance value using the formula:

$$A = \log_{10}(I_0/I_S)$$

where A is the absorbance value, I_S is the mean measured intensity (of the pixels) of the standard or sample, and I_0 is the mean measured intensity (of the pixels) of the blank.

2.3. Saliva Samples

The saliva samples used in this work were all collected from healthy volunteers in a wide range of age (20 to 40 years), by placing a 5x5 cm gauze (Wells) in the mouth for approximately two minutes. The gauze was then placed in a 5 mL syringe and squeezed in order to remove the saliva from the gauze to a 5 mL plastic tube.

The samples were diluted to half and were either used immediately (as fresh samples) or stored at -20ºC for later use (frozen samples).

2.4. Reference Procedures

In order to assess the accuracy of μPAD measurements and to validate the developed μPAD for the nitrite determination, a comparison was made between the μPAD measurements and the results obtained by performing the 4500-NO2- Colorimetric Method described in the Standard Methods for the Examination of Water and Wastewater (appendix A), since there are no reference methods for saliva analysis. All the solutions used were also prepared accordingly.

3. Results and Discussion

3.1. Preliminary Studies

As already mentioned, the Griess reaction is perhaps the most commonly known and used reaction for the determination of nitrite. However, there are several ways to prepare de Griess reagent. So, in order to obtain the best sensitivity possible, two compositions of the reagent were tested, one reported by Mesquita R. *et al.* (40), reagent A, and the other by Jayawardane Manori B. *et al.* (42), reagent B. These two reagents were tested both in a batchwise procedure (using 1 mL of reagent to 2 mL of nitrite standard; colour intensity measured in a spectrophotometer at a wavelength of 543 nm) and in filter paper (colour intensity measured through scanning), and the slopes of the resulting calibration curves are shown in Figure 14.

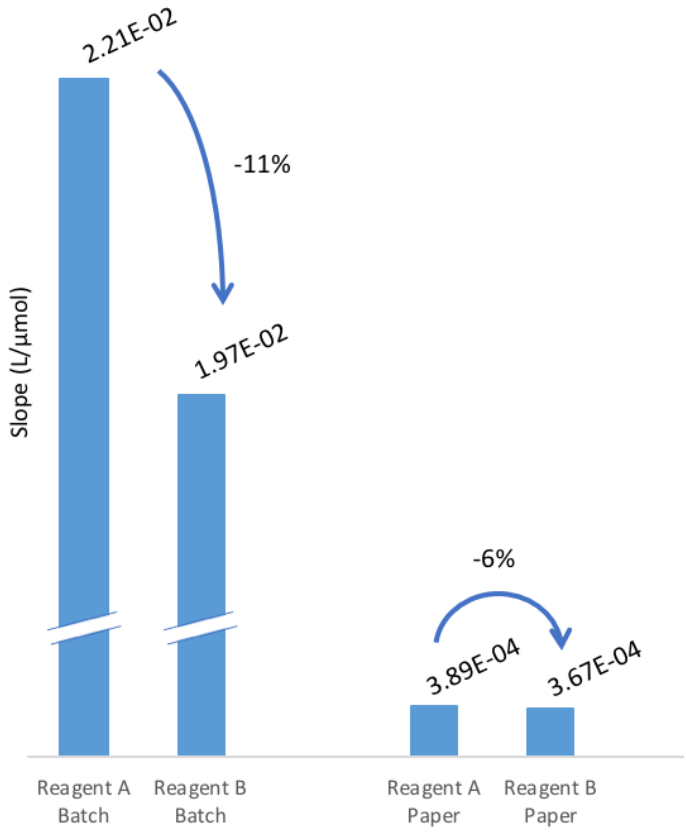

Figure 14 - Sensitivities of the calibration curves prepared using the two Griess reagents in a batchwise procedure and in paper.

After the analysis of Figure 14, the reagent A was chosen, since it presented a higher sensitivity both in a batchwise procedure and in paper.

As for the nitrate determination, in order to use the same reaction, it was necessary to reduce nitrate to nitrite. So, in reality, we are not only measuring nitrate present in the sample but nitrate plus nitrite. It is more specifically a combination of the nitrite that originated from the nitrate reduction and the nitrite naturally present in the sample. So, in order to estimate the actual concentration of nitrate in the sample, it is necessary to also know the nitrite concentration.

Three reagents, namely hydroxylamine, ascorbic acid and tin chloride, known to be reducing agents were tested alongside with the Griess reagent in a batchwise procedure. However, there was no formation of the expected pink colour, which indicated that neither of the tested reagents were able to extensively reduce nitrate to nitrite. So, it was necessary to consider an alternative; zinc has been reported by Jayawardane Manori B. *et al.* (2014) (42) to be a powerful reducing agent capable of this conversion. So, a batchwise procedure with the Griess reagent and a Zn powder (<10 µm; Sigma-Aldrich) (2 mg Zn / 2 mL standard / 1 mL of Griess reagent) was prepared to attempt to build a calibration curve and the results presented in Figure 15 confirmed that zinc was an effective reducing agent for nitrate.

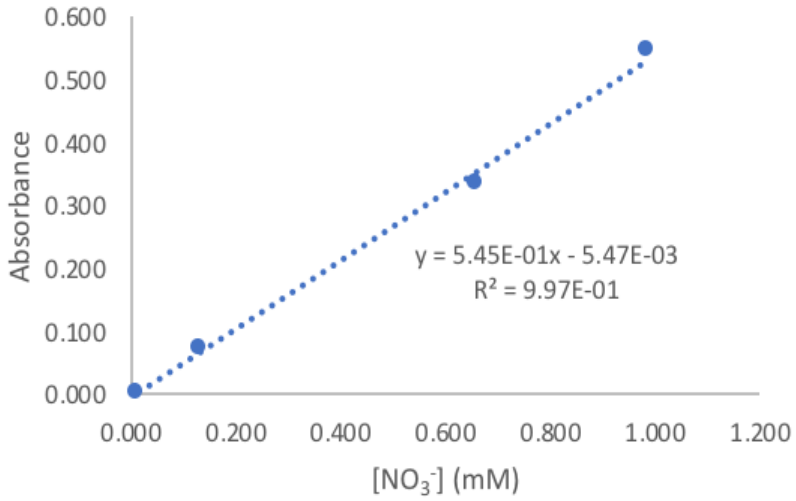

Figure 15 - Calibration curve for nitrate determination, produced by coupling the Griess reagent with zinc powder as a reducing agent.

Then the challenge became finding an efficient way of placing the zinc powder in the paper support, in order to obtain an even distribution and a sufficient amount of the said powder in the filter paper as it will be explained in section 3.3.1.

3.2. Nitrite Determination

3.2.1. Physical Design of the μPAD

After testing the reaction in a batchwise procedure and in paper, the next step was to begin developing the physical structure of the μPAD. For the hydrophobic area a plastic laminating pouch was chosen, and for the hydrophilic areas, where it would occur the reaction, 24 filter paper disks were used (24 areas of measurement per μPAD). Since there is only one reagent needed to do the nitrite determination, first a μPAD with only one layer of filter paper disks containing the Griess reagent was prepared. However, because the reagent was in direct contact with the air through the sample insertion hole, it oxidized very easily. Moreover, one layer allowed a very limited volume of sample (10 μL maximum) and it took a long time to absorb that same volume (30 minutes minimum for 10 μL). So, an empty layer (with no reagent) was added on top of the reagent layer in order to protect it from oxidation and also to allow the placement of a higher volume of sample with a smaller absorption time. In this 2-layers μPAD, the same 10 μL of sample was completely absorbed in under 5 minutes.

3.2.2. Study of the Influence of the Filter Paper

There is available in the market several types of filter paper with different treatments and poor diameters (Appendix B). In order to choose the best paper for the layers of the μPAD, a few different types of paper were tested.

Since the bottom layer was the only layer that was intended to have a reagent, that reagent (10 μL) was tested in the Whatman filter papers nº 1, 42, 50 and 541. One 1-layer μPAD consisting on 4 rows, one for each type of paper, was prepared. Each row had 6 disks. In 3 of them was placed water (10 μL) as the blank, and in the other 3 was placed a 20 μM standard (10 μL). The pixels intensities in the image of the scanned μPAD, were converted to the absorbance values shown in Figure 16.

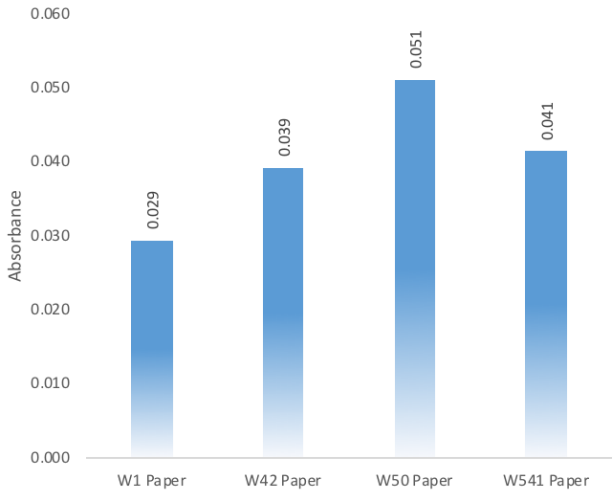

Figure 16 – Absorbance values of a 20 µM standard using four different types of paper.

The Whatman 50 paper was the one chosen, as it presented a higher absorbance value. Next, a 2-layer µPAD was prepared, both of the layers with W50 paper (10 µL of reagent). A good calibration curve was obtained but the µPAD needed at least 30 minutes to absorb the 15 µL of standards. This could be justified by the small porosity of this type of paper. So, to improve the sensitivity and reduce the µPAD drying time, the Whatman filter papers n. º 1, 5, 42 and 50 were used for the top empty layer and combined with the W50 paper in the reagent layer. The resulting sensitivities of the calibration curves are presented in Figure 17.

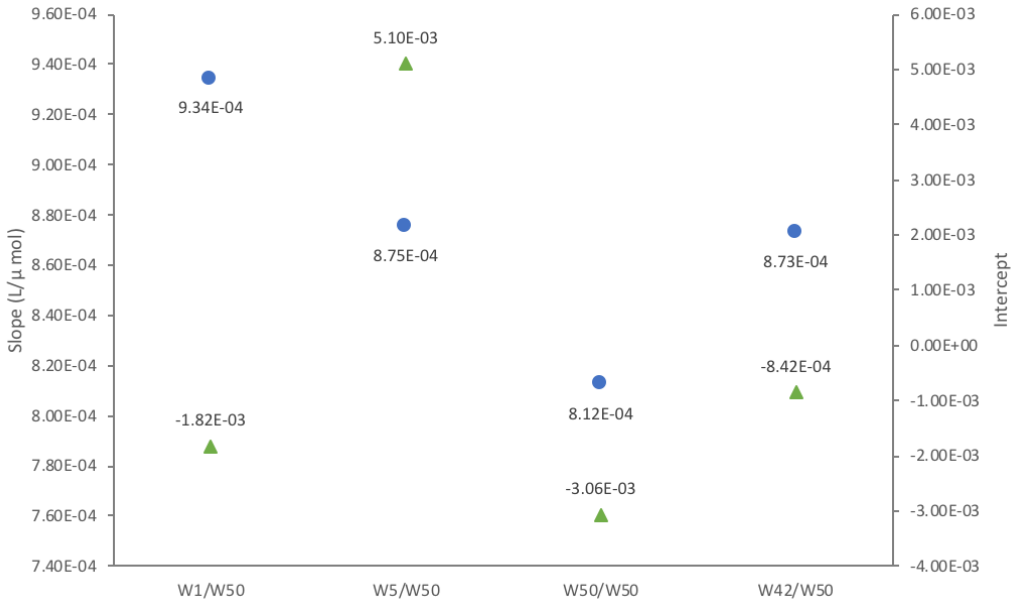

Figure 17 – Study of the influence of different types of filter paper in the first layer on the nitrite µPAD (● Slope; ▲ Intercept).

After analysing the results, the Whatman 1 as the top layer paper of the µPAD was the option that produced a calibration curve with the higher sensitivity and the second intercept closer to zero. This structure of W1/W50 was also the one that allowed the µPAD scanning in least amount of time of all the paper studied (scanning in 20 minutes). For these reasons, Whatman 1 was chosen as the more adequate filter paper for the top layer of the µPAD, when combined with the Whatman 50 for the reagent layer.

3.2.3. Study of the Influence of the Reagent Volume

The next step on optimizing the µPAD for the nitrite determination was to study the optimal volume of Griess reagent to place on the bottom layer of the µPAD. After doing a preliminary test of the volume capacity of these paper disks (9.5 mm diameter, Whatman 50), it was observed that, in order to obtain an even distribution of the reagent on these paper disks, the volume had to be higher than 5 µL per disk. As for the maximum capacity of the disks, it presented to be approximately 12 µL. Therefore, the reagent volumes studied were 5 and 10 µL and the slope and intercept that resulted from those calibration curves are present in Figure 18.

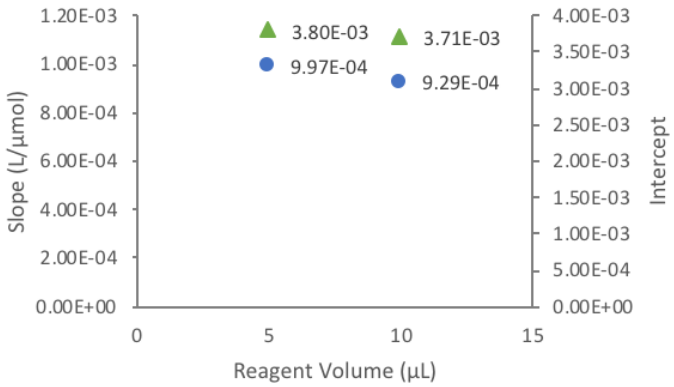

Figure 18 - Study of the influence of the reagent volume in the nitrite µPAD (● Slope; ▲ Intercept).

Comparing the results of both volumes studied, it was possible to state that there is no significant difference (<10%) either between the sensitivities or the intercepts. So, to avoid the unnecessary consumptions of reagents, 5 µL of Griess reagent per paper disk was chosen for the bottom layer of the nitrite µPAD.

3.2.4. Study of the Influence of Sample Volume

The last parameter tested to optimize the µPAD was the sample volume. To do this study, calibrations curves were prepared on the µPADs by inserting three different sample/standard volumes, namely 10, 15 and 20 µL. The resulting sensitivities and intercepts of this study are presented in Figure 19.

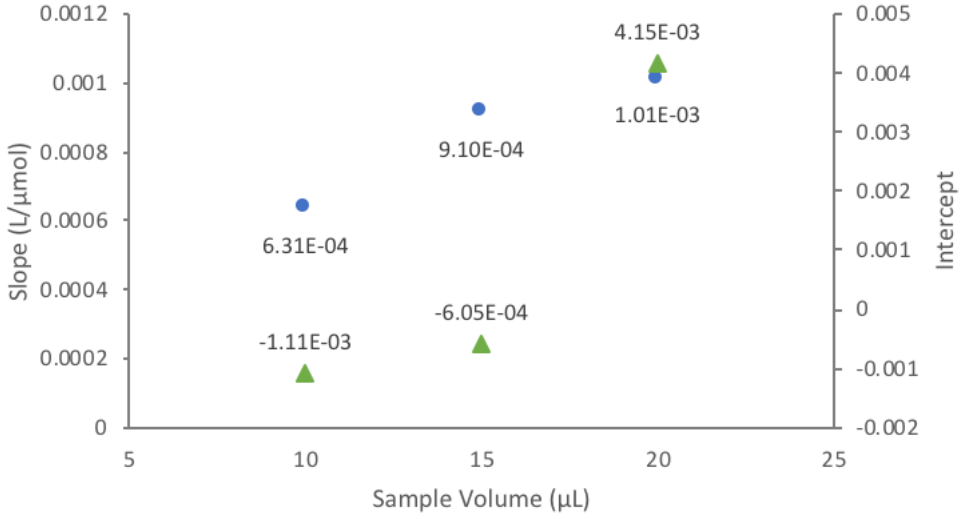

Figure 19 - Study of the influence of the sample volume in the nitrite µPAD (● Slope; ▲ Intercept).

When using either 10 or 15 µL, the sample was completely absorbed in approximately 15 minutes. When applied 20 µL of sample, it took about 35 minutes for the µPAD to completely absorb that sample/standards. Although the highest sensitivity was achieved using the 20 µL of sample, the chosen sample volume was the 15 µL, as a compromise solution between sensitivity and absorption time.

3.3. Nitrate Determination

3.3.1. Physical Design of the µPAD

The nitrite determination can be accomplished either by using simultaneous or sequential methods. Since a µPAD for nitrite determination had already been developed, the sequential methodology was chosen for nitrate determination by using the nitrite µPAD and adapting it for nitrate determination. After testing different reducing agents in a batchwise

procedure and choosing zinc powder as the reducing agent, as described previously in the preliminary tests (section 3.1), the difficulty became placing that powder in the paper, mainly because either the amount of zinc placed was not enough or the distribution of the powder was not even. Even though several procedures were tested, the best one consisted in placing the filter paper disks in a zinc suspension (1 g of zinc powder in 20 mL of water), stir the suspension manually and then remove and dry the disks in a 50ºC oven for 30 minutes.

Since one of the layers of the nitrite µPAD developed was empty, it was thought to use that layer for the placement of the zinc powder. However, the direct contact of the zinc on the top layer with the Griess reagent on the bottom layer caused a visible degradation of the reagent, even before the sample/standard insertion, as illustrated in Figure 20A. In order to separate the two layers and prevent the Griess reagent degradation, another layer of filter paper was added between the zinc and the Griess reagent. To ensure that there was absolutely no contact, this new layer consisted in a Whatman 1 filter paper disk with a bigger diameter (1.27 cm diameter) than the other layers. As it can be seen in Figure 20B, this modification entirely prevented the reagent degradation. Considering that the only purpose of this middle layer was to serve as a physical barrier, it wasn't tested other types of filter paper.

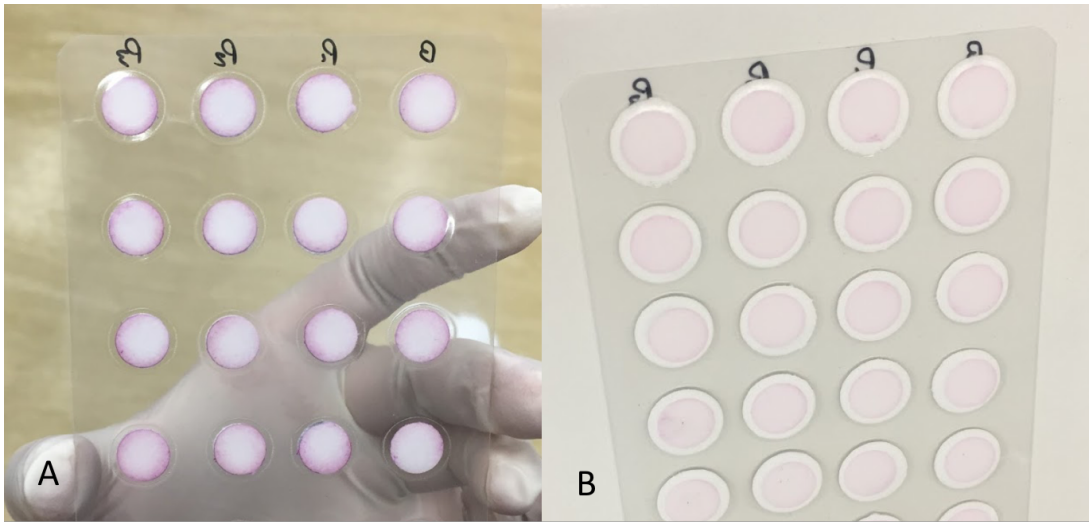

Figure 20 - (A) 2-layer µPAD for nitrate determination; (B) 3-layer µPAD for nitrate determination.

After the standard insertion on the µPADs, it was observed that, because this structural prevented the degradation of reagent, it also significantly improved the quality of the calibration curves produced. Initially, because of the reagent degradation, it was not possible at all to produce a viable calibration curve. With the addition of the middle layer, and consequently the protection of the Griess reagent, the intensity of the pink consistently

increased with the concentration of nitrate, which made it possible to build a viable calibration curve. The difference between the coloured product in the µPADs before and after the addiction of the middle layer is shown in Figure 21 and the calibration curve produced with the 3-layer µPAD is presented in Figure 22.

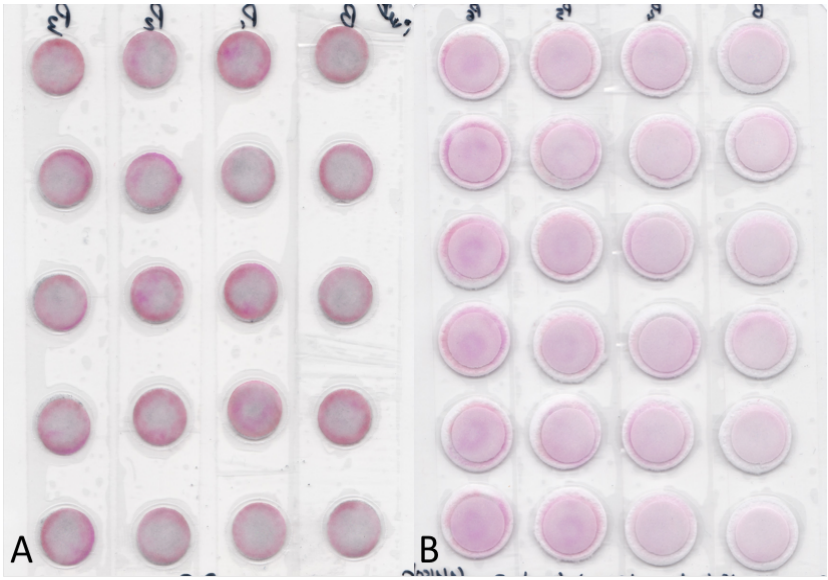

Figure 21 - (A) 2-layer µPAD scan after the placement of three different standards; (B) 3-layer µPAD scan after the placement of three different standards.

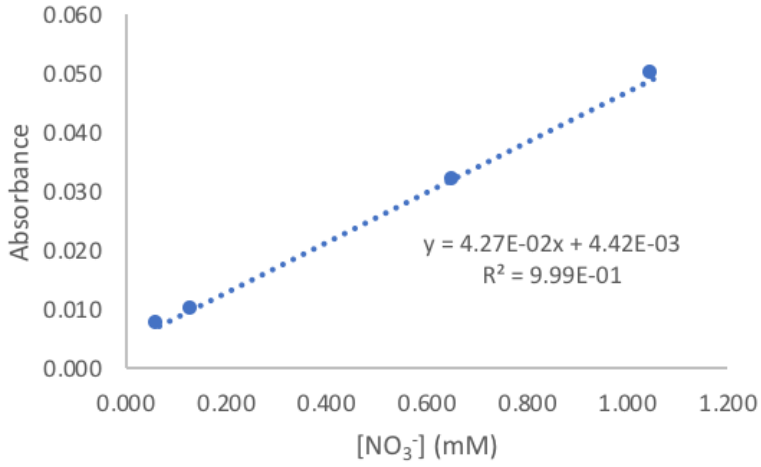

Figure 22 – Nitrate calibration curve obtained with the 3-layer µPAD

So, after making the alterations to adapt the developed nitrite µPAD to the nitrate determination, the physical structure of the said µPAD consisted of 3 layers of paper (W1/W1/W50), in which the first layer contained the zinc powder, the middle and larger layer remained empty, and the bottom layer supported the Griess reagent.

3.3.2. Study of the Influence of the Reagent Volume

After establishing the modifications of the physical structure of the µPAD, and because the studied range of the nitrate concentration is higher than the nitrite concentrations, the influence of the reagent volume was studied again. The same volumes of 5 and 10 µL were tested, for the same reasons indicated before. The sensitivities of the resulting calibration curves are presented in Figure 23.

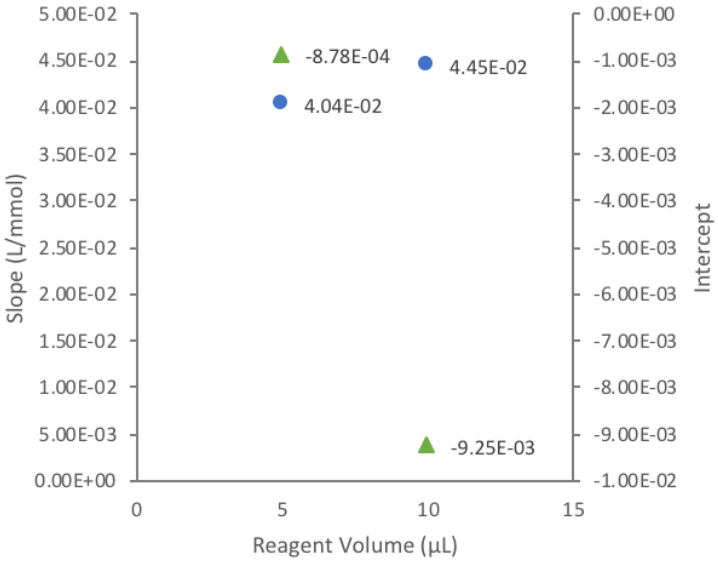

Figure 23 - Study of the influence of the reagent volume in the nitrate µPAD (● Slope; ▲ Intercept).

As shown in Figure 23, the use of 10 µL of Griess reagent produced a 10% increase of the sensitivity, which is considered a significant difference, when compared with the 5 µL. Therefore, the chosen volume to be used on the nitrate µPAD was 10 µL of the Griess reagent.

3.3.3. Study of the Influence of the Sample Volume

Because a third layer of paper was introduced in the µPAD, the µPAD absorption capability increased significantly. With the same volume of sample applied, the amount of sample that reaches the reagent is smaller in a 3-layers µPAD when compared with a 2-layer µPAD, because part of that sample is held in the first layers. Therefore, it was important to study several sample volumes, and choose the volume that allows a higher sensitivity.

The sample volumes tested were 15, 20, 25 and 30 µL. With the first three volumes the sample was completely absorbed into the µPAD almost immediately, but when 30 µL of sample was used, it took about 35 minutes to observe the sample absorption. Since 35 minutes was considerate too much time, the option of 30 µL of sample was excluded from the study.

As for the remaining volumes, even though it was possible to scan the µPAD almost immediately after placing the sample, it was observed that for the first 20 minutes the sensitivities increased exponentially. This is due to the fact that the conversion of nitrate to nitrite slows down the colour reaction, which in turn justify the slower increase of the colour product intensity and consequently the increase of the sensitivity. So, to compare the effect of the sample volume, sensitivities of the calibration curves for a scanning time of 20 minutes are presented in Figure 24.

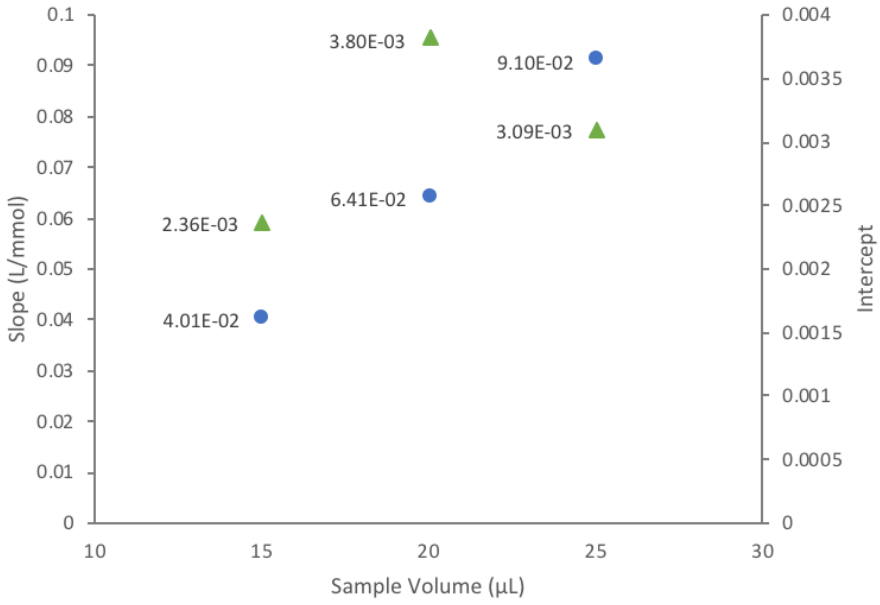

Figure 24 - Sample volume study for the nitrate determination µPAD (● Slope; ▲ Intercept).

As shown on the results in Figure 24, out of the three volumes (15, 20 and 25 µL), the one that presented the calibration curve with the highest sensitivity was without a doubt the 25 µL of sample. This volume also allowed a quick scanning of the µPAD which is why it was chosen as the ideal sample volume for the nitrate µPAD.

3.4. Interferences Assessment

To study the interference of the saliva matrix, two calibration curves for each µPAD (nitrite and nitrate) were prepared by using either standards in water, or in synthetic saliva. The synthetic saliva prepared ([KCl] = 2237 mg/L; [KH_2PO_4] = 544.3 mg/L; [HEPES] = 4766 mg/L; [$CaCl_2.2H_2O$] = 77.69 mg/L; [MgCl] = 19.04 mg/L; [Bovine Serum Albumin] = 2700 mg/L) was based on the concentrations reported by Batista G. *et al.* (43). The sensitivity values of the resulting calibration curves are represented in Figure 25.

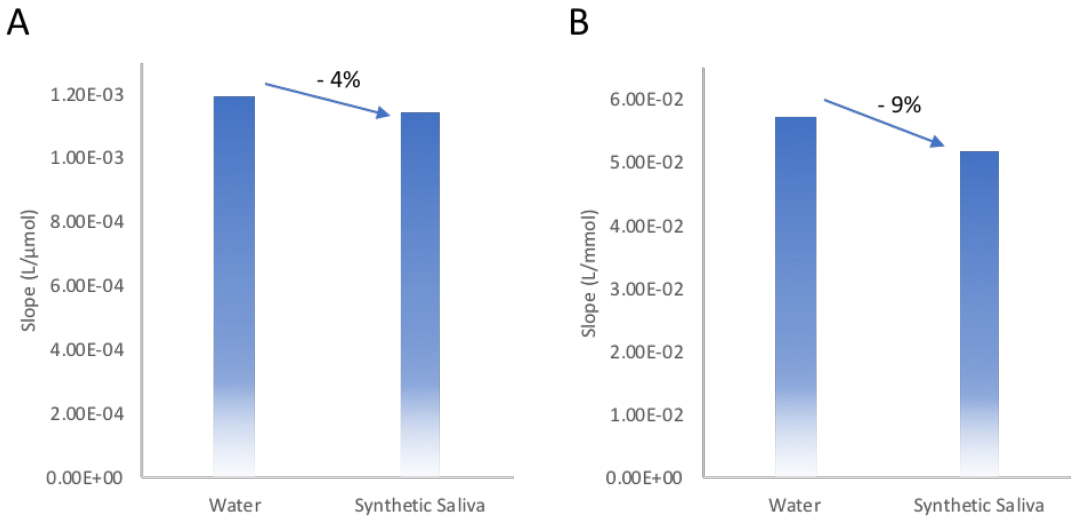

Figure 25 - (A) Comparison of the sensitivities of the calibration curves prepared with water and synthetic saliva standards in the nitrite µPAD; (B) Comparison of the sensitivities of the calibration curves prepared with water and synthetic saliva standards in the nitrate µPAD.

For both nitrite (Figure 25A) and nitrate (Figure 25B) determination, the use of synthetic saliva standards revealed no significant difference on the sensitivity of the calibration curves, since the variation observed was inferior to 10%. Therefore, to simplify the process and to reduce the reagents consumption, it was chosen to maintain the use of standards prepared in water, for both the nitrite and nitrate determination µPADs.

3.5. Stability Studies

In order to evaluate the robustness of the developed µPADs, stability studies were designed and performed to test the stability of these microfluidic devices not only when stored, before the sample insertion, but also to evaluate the stability of the coloured product formed after the sample insertion.

3.5.1. Stability of the Coloured Product

To evaluate the stability of coloured product in both of the developed nitrite and nitrate µPADs, a calibration curve for each µPAD was prepared. These µPADs were scanned several times after the standards insertion, up until 4 hours. The sensitivities of the calibration curves scanned during the 4 hours are represented in the Figures 26 and 27, for the nitrite µPAD, and Figures 28 and 29, for the nitrate µPAD. A range of ±10% (or ±5%) of the sensitivity of the first scanned calibration curve is also represented in order to facilitate the evolution analysis.

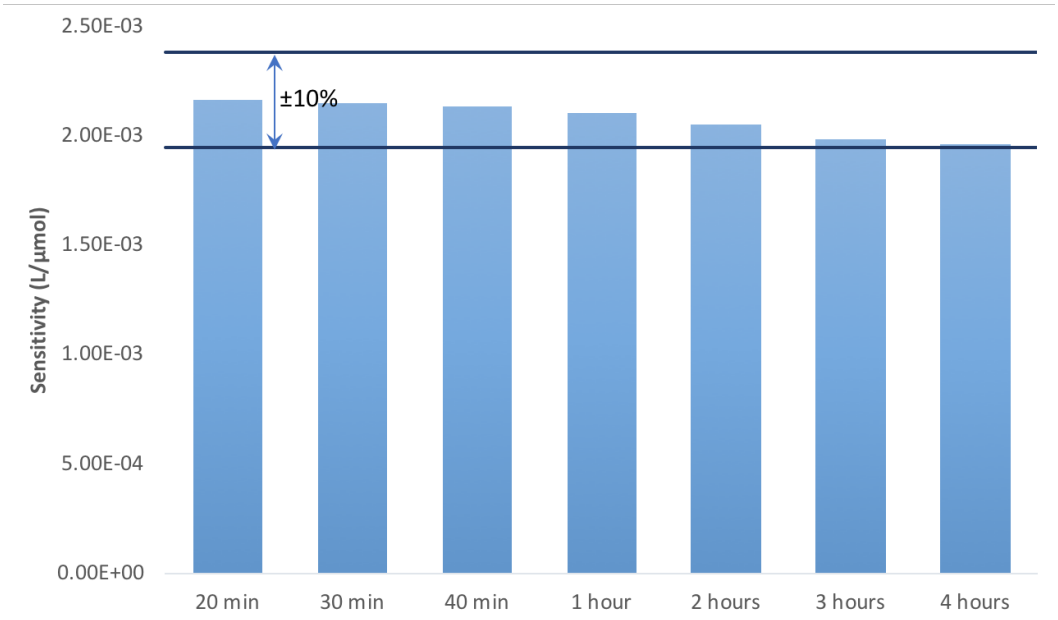

Figure 26 - Stability of the coloured product in the nitrite µPAD considering a variation range of ±10%.

After analysing Figure 26, it is possible to conclude that the sensitivity provided by scanning the µPAD 20 minutes after applying the standards, continually decreases over time and considering a variation range of ±10%, there is no significant difference between scanning the µPAD at 20 minutes or at 4 hours after the standards insertion. However, when considering a range of ±5% (Figure 27), the maximum time in which the sensitivity stays within the range is 2 hours.

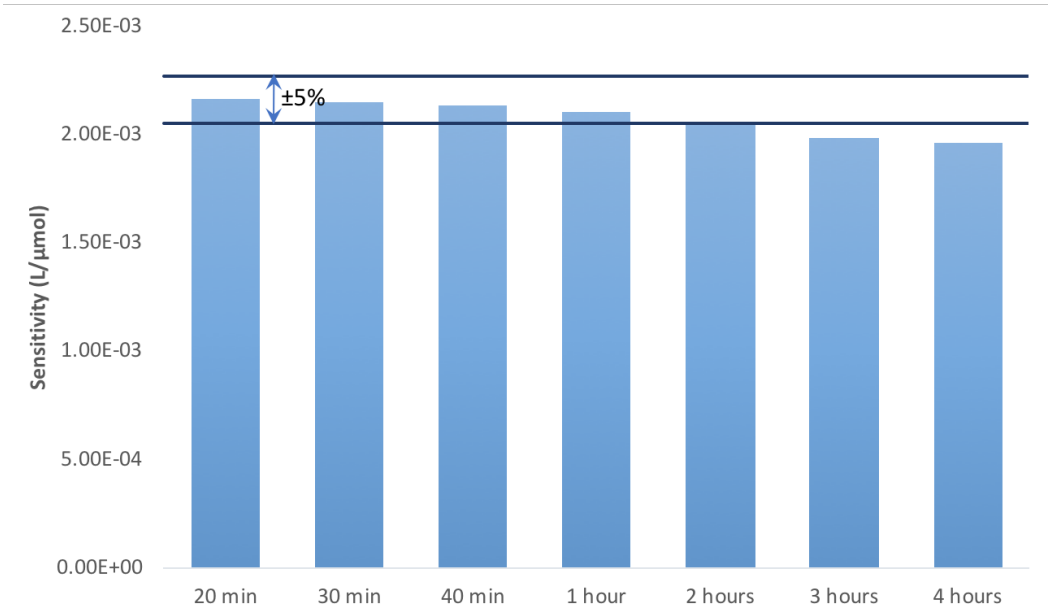

Figure 27 - Stability of the coloured product in the nitrite µPAD considering a variation range of ±5%.

As for the nitrate determination µPAD (Figures 28 and 29), unlike what was observed with the nitrite µPAD, initially there was an increase in the sensitivity up until 1 hour. This can be justified not only by the existence of an extra layer, but also the existence of a reduction reaction before the colour reaction, both of which slow down the formation of the pink coloured product.

After reaching a maximum slope at 1 hour, the sensitivity begins to decrease up until the tested 4 hours. Although there is an increase of sensitivity in the first hour, it is not statistically significant when considering a ±10% range, as shown in Figure 28. Whereas, if the µPAD is scanned 3 hours or more after the standards placement, the sensitivity obtained is significantly lower than the one obtained up until the 2 hours.

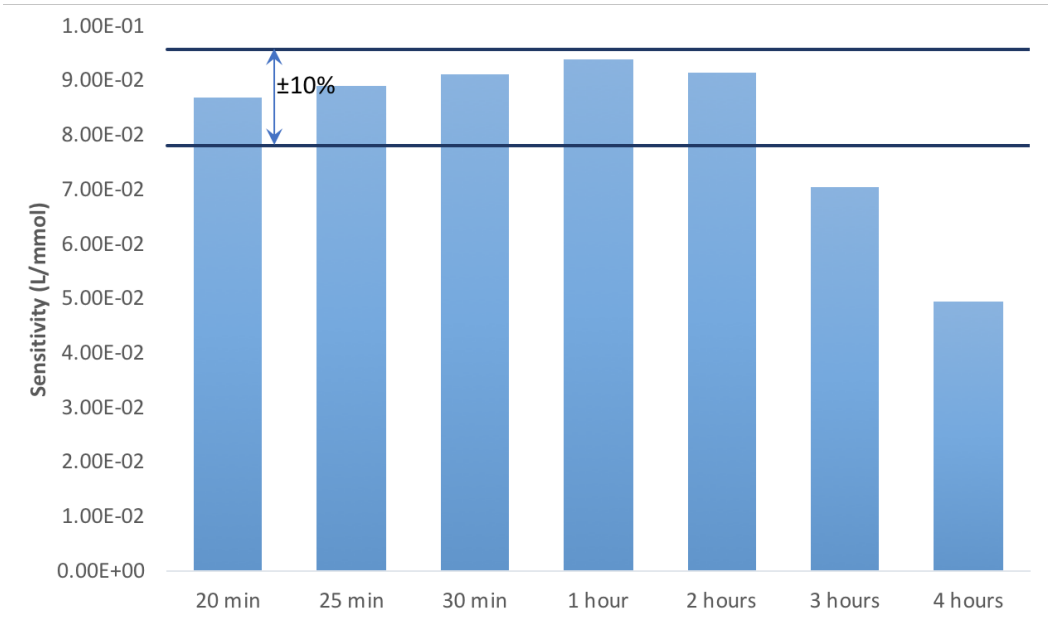

Figure 28 - Stability of the coloured product in the nitrate µPAD considering a variation range of ±10%.

However, if a range of ±5% is considered, as represented in Figure 29, then the sensitivity obtained 1 hour after the standards insertion is considered significantly higher than the remaining sensitivities obtained.

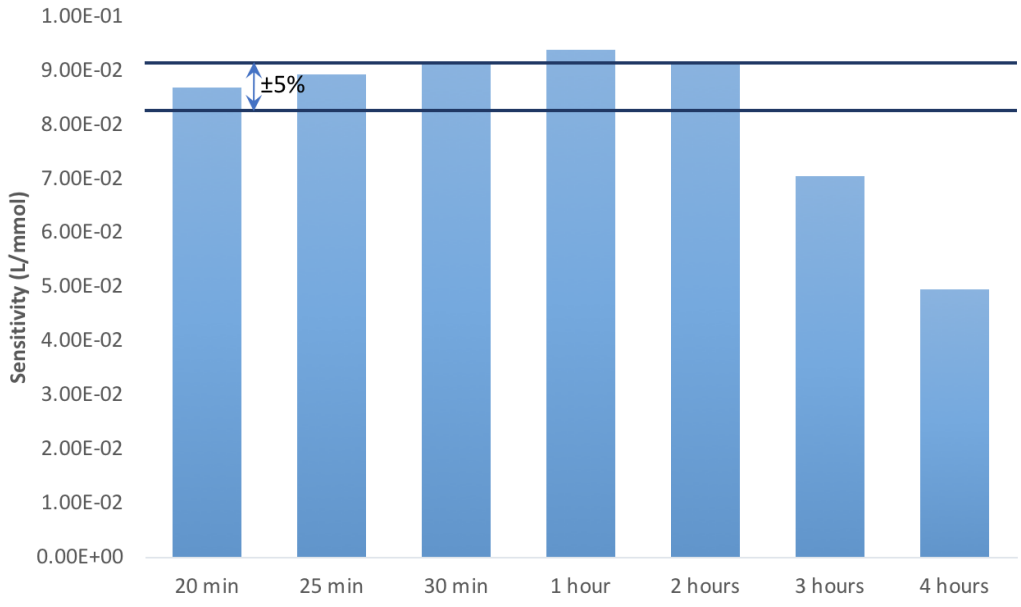

Figure 29 - Stability of the coloured product in the nitrate µPAD considering a variation range of ±5%.

3.5.2. µPAD's Stability

To test the stability of the µPADs before the sample insertion, these devices were prepared and then stored under three different atmospheric conditions (air, nitrogen, and vacuum). The µPADs tested in air atmosphere were stored in a closed clear zip lock bag. The µPADs tested in nitrogen atmosphere were stored in a closed clear zip lock bag that was field with nitrogen for approximately 1-2 minutes. The µPADs tested in a vacuum were also stored in a closed clear zip lock bag, in which the air was removed using a vacuum pump. It is also important to refer that all µPAD's were shielded from the light when stored, regardless of the atmospheric condition they were under. Each of the atmospheric conditions were also tested for three different periods of time: overnight (1 day), overweekend (3 days) and overweek (7 days). Every time the µPADs were removed from storage, a set of standards were inserted on that µPAD in order to build a calibration curve. On that same day, another calibration curve was prepared using the same set of standards, on freshly assembled µPADs. The average sensitivity of these calibration curves was then compared with the sensitivities of the µPAD's under the different conditions. A variation under 10% of the average calibration curves was considered a non-significant difference and, in order to facilitate the results analysis, this range of ±10% was represented in the figures. The results for the nitrite determination µPAD are presented in Figure 30.

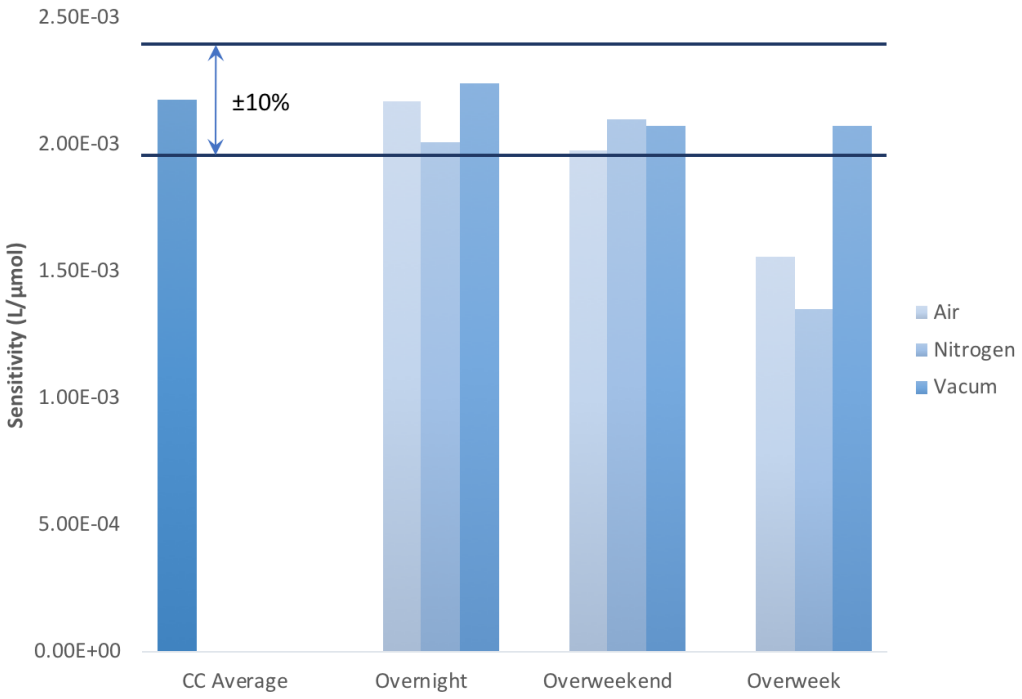

Figure 30 – Nitrite µPAD stability results considering a variation range of ±10%.

As it can be observed in Figure 30, after one day of storage (overnight), the designed µPAD for the nitrite determination showed no significant difference, in all types of storage, when compared with the freshly prepared calibration curves. The same happened with the 3 days storage (overweekend). As for the overweek results (7 days), the only type of storage that maintained the µPAD sensitivity, showing no significant difference from the daily calibration curves, was the vacuum storage.

The stability results for the nitrate determination µPAD are shown in Figure 31.

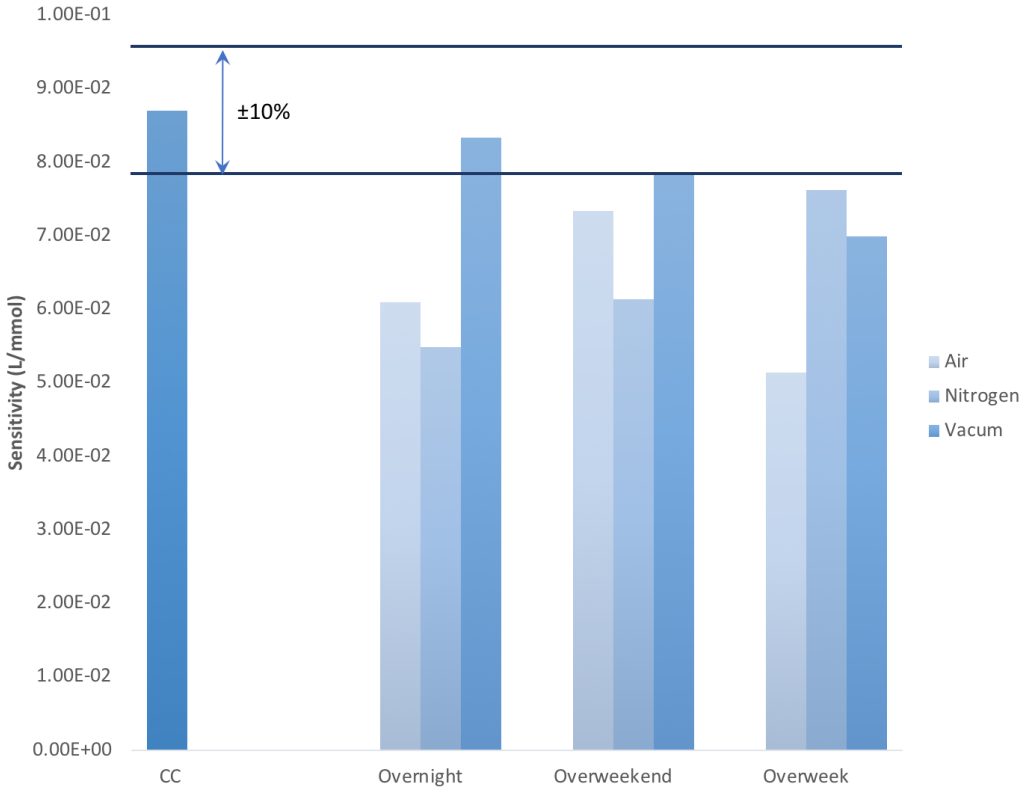

Figure 31 - Nitrate µPAD stability results considering a variation range of ±5%.

After analysis of the nitrate µPAD' stability results, it is possible to conclude that neither the air atmosphere, nor the nitrogen atmosphere were able to appropriately preserve the µPAD for none of the periods of time tested, which is justified by the decrease of the calibration curves sensitivities below the acceptable ±10% range. As it can be verified in Figure 31, the vacuum storage was the only one that was able maintain the quality of the calibration curves, although only for a maximum of 3 days of storage (overweekend).

So, the µPAD designed for the nitrite determination maintained its quality of measurement, when stored with vacuum, for at least a week, although more tests would be

required to analyse the stability for more than 7 days. After the sample/standard placement, the scanning of the µPAD can be executed within 4 hours, since it was shown that, considering a ±10% range of variation, no significant differences were found between the sensitivities obtained.

As for the nitrate determination µPAD, it has to be stored with vacuum for a maximum of 3 days to provide the same quality of results as a freshly prepared µPAD. When the sample/standard is inserted, the scanning of the µPAD as to be executed within 2 hours, in order to maintain the consistency of the measurement quality, assuming a ±10% range of variation.

3.6. Analytical Features

The main characteristics of the developed µPAD such as dynamic range, average calibration curve, limits of detection (LOD) and quantification (LOQ), relative standard deviation (RSD) and the µPAD's optimal scanning time range, are presented in Table 2.

Table 2 - Features of the developed µPADs for the determination of nitrite and nitrate; Limit of Detection (LOD); Limit of Quantification (LOQ); Relative Standard Deviation (RSD)

Analyte	Dynamic range	Calibration curve* A = S x [NO_x] + b	LOD*	LOQ*	RSD*	Scanning Time
Nitrite	5 - 45 µM	$y = 1.78 \times 10^{-3}(\pm 5.60 \times 10^{-5}) \times [NO_2^-] + 1.12 \times 10^{-3}(\pm 3.08 \times 10^{-5})$ $R^2 = 0.997$	0.05 µM	0.17 µM	3.1%	20 min – 4 h
	45 - 220 µM	$y = 1.12 \times 10^{-3}(\pm 3.05 \times 10^{-5}) \times [NO_2^-] + 3.21 \times 10^{-2}(\pm 2.57 \times 10^{-3})$ $R^2 = 0.996$				
Nitrate	0.2 - 1.2 mM	$y = 7.27 \times 10^{-2}(\pm 8.35 \times 10^{-3}) \times [NO_3^-] - 2.63 \times 10^{-3}(\pm 1.93 \times 10^{-3})$ $R^2 = 0.988$	0.08 mM	0.27 mM	11%	20 min – 2 h

*n=6, being n the number of calibration curves used for the calculations.

After gathering several nitrite calibrations curves, it was observed that within the working concentration range of 5 – 220 µM, there was different sensitivities. Therefore, this

concentration range was divided in two, the range of 5 to 45 µM and the range of 45 to 220 µM, being the 45 µM the point of interception.

The limit of detection (LOD) and limit of quantification (LOQ) were calculated as concentration corresponding to three or ten-times, respectively, the standard deviation of the intercept, according to IUPAC recommendations (44).

The reproducibility of the developed µPADs was evaluated using the relative standard deviation (RSD). The RSD was calculated by dividing the standard deviation of the typical calibration slope by the average slope of that calibration curve.

3.7. Costs Analysis

As it was mentioned several times before, the purpose of this work was to develop two µPADs the determination of nitrite and nitrate in human saliva.

To know the cost of each of the µPAD's developed, in was taken into account all the consumables necessary for their assembly, namely, the price of paper, the price of reagents and the price of plastic laminating pouches. The cost of each type of consumables for one of each type of µPAD is discriminated in Table 3.

Table 3 - Cost of the consumables for each µPAD and total cost of one µPAD for each determination.

µPAD	Filter Paper		Reagents		Plastic Pouch	Total Cost per µPAD
	Whatman 1	Whatman 50	Griess Reagent	Zinc Powder		
Nitrite	0.022€	0.071€	0.0047€	-	0.046€	≈ 0.15€
Nitrate	0.058€	0.071€	0.0094€	0.0097€	0.046€	≈ 0.20€

To assemble one nitrite µPAD, it is necessary 24 Whatman 1 paper disks of 9.5 mm diameter, 24 Whatman 50 paper disks of 9.5 mm diameter, 120 µL of Griess reagent (5 µL/W50 disk) and one plastic pouch, which makes up for a total of approximately 0.15€ per µPAD.

To assemble one nitrate µPAD, it is necessary 24 Whatman 1 paper disks of 9.5 mm diameter, 24 Whatman 1 paper disks of 1.27 cm diameter, 24 Whatman 50 paper disks of 9.5

mm diameter, 240 µL of Griess reagent (10 µL/W50 disk), a zinc suspension of approximately 1 g/20 mL and one plastic pouch, which makes up for a total of approximately 0.20€ per µPAD. The cost calculations are presented in more detail in appendix C.

3.8. Application of the Developed µPADs

3.8.1. Comparison with Reference Procedure using Saliva Samples

With the µPAD completely developed and optimized, it was necessary to proceed to the validation of this developed method. To achieve this validation, sample measurements were performed both using the nitrite µPAD and the 4500-NO2- Colorimetric Method described in the Standard Methods for the Examination of Water and Wastewater (Appendix A), and the results (Appendix D) were compared and represented in Figure 32.

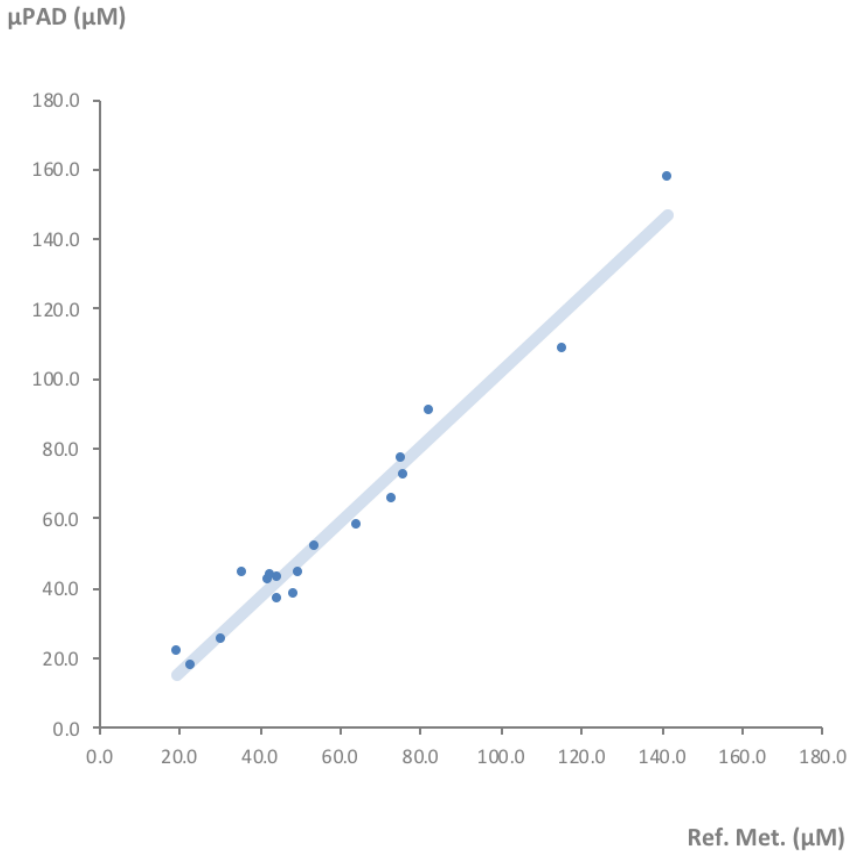

Figure 32 – Comparison between the developed nitrite µPAD and the colorimetric reference methods.

As in can be observed in Figure 32, the 18 samples collected from healthy volunteers, were dispersed along a width range of concentrations that showed to be within the range tested since the beginning of this work. It is also possible to observe that these measurements line up in a straight line, forming a trendline: y = 1.08 (±0.11) x - 5.58 (±7.20). Statistically speaking, in order to say that there is no significant difference between the two methods, the slope range of the trendline has to include the value 1 and the intercept range has to include the value 0. Since the slope range obtained was [0.97; 1.19] and the intercept range was [-12.78; 1.62], it is possible to conclude that there are no significant statistical differences between the reference procedure and the developed μPAD for the nitrite determination.

4. Conclusions and Suggestions for Future Work

The focus of this work was to develop two new microfluidic paper-based analytical devices (μPADs) for the nitrite and nitrate detection and quantification in human saliva samples. The main application envisioned for these devices was for them to facilitate the diagnosis of some diseases and health conditions, not only in healthcare facilities but also in remote areas.

According to the World Health Organization, population living in developing countries commonly don't have access to the basic health care, either because these countries don't have the resources, because of geographical difficulties or because the treatments are too expensive to be accessible. Another challenge found in these countries is the lack of skilled professional to perform the tests, especially in the most secluded areas. In order to minimize these problems, researchers have been working on the development of devices and techniques, that according to the World Health Organization should be "Affordable, Sensitive, Specific, User-friendly, Rapid and Robust, Equipment-free, and Deliverable to end-users".

The final structure of developed μPADs, both for the nitrite and nitrate determination, were the result of several optimization studies. The nitrite μPAD final structure was composed by two layers of filter paper. The bottom layer consisted of 9.5 mm diameter disks of Whatman 50 filter paper with 5 μL of Griess reagent and the top layer of 9.5 mm diameter empty disks of Whatman 1 filter paper. The nitrate μPAD final structure was composed by three layers of filter paper. The bottom layer consisted of 9.5 mm diameter disks of Whatman 50 filter paper with 10 μL of Griess reagent, the middle layer consisted of 1.27 cm diameter empty disks of Whatman 1 filter paper and the top layer consisted of 9.5 mm diameter disks of Whatman 1 filter paper with zinc powder.

Since one of the aims of this work was to use these devices in saliva samples, an interference assessment using synthetic saliva standards was performed. Because the variation between the water and saliva calibration curves sensitivities was under 10%, it was possible to conclude that the saliva matrix didn't interfere with the measurements provided by both of the developed μPADs.

To confirm the μPAD's applicability in on-location measurements, these devices were submitted to stability studies, both before and after the sample insertion. The nitrite μPAD presented itself stable when stored in vacuum for 7 days (maximum duration tested) and, when applied the sample or standard, the coloured product was stable for 4 hours, providing measurements with no significant variability. The μPAD for nitrate determination presented itself stable only when stored in vacuum and for a maximum of 1 day. When applied the

sample or standard, the coloured product was stable for 2 hours, providing measurements with no significant variability.

Finally, to validate this method, nitrite μPAD measurements of several samples were compared with the measurements obtained from performing the colorimetric method described in Standard Methods for the Examination of Water and Wastewater and the results showed no statistically significant differences between the measurements obtained from the two methods.

In conclusion, the developed μPADs for nitrite and nitrate determination exhibited promising properties in saliva samples, possibly for the use in remote locations, since they are sensitive, portable and user-friendly, and provide rapid measurements without needing complex equipment or specialized technicians in the field. These devices are also environmental-friendly, since they are disposable by incineration, and affordable, having a cost of 0.15€ and 0.20€ per μPAD of nitrite and nitrate, respectively.

As future work, it would be interesting to validate the μPAD developed for the nitrate determination, to test both of the μPAD's stability for a longer period of time and in different storage conditions than the ones studied, and also to perform field studies to further access the impact of conditions different from the ones that exist in the laboratory. Ultimately, the μPADs should be used for analysis in saliva samples of patients with NO_X-related diseases.

Appendix

A. 4500-NO2- Colorimetric Method - Standard Methods for the Examination of Water and Wastewater

4500-NO_2^- B. Colorimetric Method

1. General Discussion

a. Principle: Nitrite (NO_2^-) is determined through formation of a reddish purple azo dye produced at pH 2.0 to 2.5 by coupling diazotized sulfanilamide with *N*-(1-naphthyl)-ethylenediamine dihydrochloride (NED dihydrochloride). The applicable range of the method for spectrophotometric measurements is 10 to 1000 µg NO_2^--N/L. Photometric measurements can be made in the range 5 to 50 µg N/L if a 5-cm light path and a green color filter are used. The color system obeys Beer's law up to 180 µg N/ L with a 1-cm light path at 543 nm. Higher NO_2^- concentrations can be determined by diluting a sample.

b. Interferences: Chemical incompatibility makes it unlikely that NO_2^-, free chlorine, and nitrogen trichloride (NCl_3) will coexist. NCl_3 imparts a false red color when color reagent is added. The following ions interfere because of precipitation under test conditions and should be absent: Sb^{3+}, Au^{3+}, Bi^{3+}, Fe^{3+}, Pb^{2+}, Hg^{2+}, Ag^+, chloroplatinate ($PtCl_6^{2-}$), and metavanadate (VO_3^{2-}). Cupric ion may cause low results by catalyzing decomposition of the diazonium salt. Colored ions that alter the color system also should be absent. Remove suspended solids by filtration.

c. Storage of sample: Never use acid preservation for samples to be analyzed for NO_2^-. Make the determination promptly on fresh samples to prevent bacterial conversion of NO_2^- to NO_3^- or NH_3. For short-term preservation for 1 to 2 d, freeze at –20°C or store at 4°C.

2. Apparatus

Colorimetric equipment: One of the following is required:

a. Spectrophotometer, for use at 543 nm, providing a light path of 1 cm or longer.

b. Filter photometer, providing a light path of 1 cm or longer and equipped with a green filter having maximum transmittance near 540 nm.

3. Reagents

a. Nitrite-free water: If it is not known that the distilled or demineralized water is free from NO_2^-, use either of the following procedures to prepare nitrite-free water:

1) Add to 1 L distilled water one small crystal each of $KMnO_4$ and either $Ba(OH)_2$ or $Ca(OH)_2$. Redistill in an all-borosilicate-glass apparatus and discard the initial 50 mL of distillate. Collect the distillate fraction that is free of permanganate; a red color with DPD reagent (Section 4500-Cl.F.2*b*) indicates the presence of permanganate.

2) Add 1 mL conc H_2SO_4 and 0.2 mL $MnSO_4$ solution (36.4 g $MnSO_4 \cdot H_2O$/100 mL distilled water) to each 1 L distilled water, and make pink with 1 to 3 mL KMnO4 solution (400 mg $KMnO_4$/ L distilled water). Redistill as described in the preceding paragraph.

Use nitrite-free water in making all reagents and dilutions.

b. Color reagent: To 800 mL water add 100 mL 85% phosphoric acid and 10 g sulfanilamide. After dissolving sulfanilamide completely, add 1 g *N*-(1-naphthyl)-ethylenediamine dihydrochloride. Mix to dissolve, then dilute to 1 L with water. Solution is stable for about a month when stored in a dark bottle in refrigerator.

c. Sodium oxalate, 0.025*M* (0.05*N*): Dissolve 3.350 g $Na_2C_2O_4$, primary standard grade, in water and dilute to 1000 mL.

d. Ferrous ammonium sulfate, 0.05*M* (0.05*N*): Dissolve 19.607 g $Fe(NH_4)_2(SO_4)_2 \cdot 6H_2O$ plus 20 mL conc H_2SO_4 in water and dilute to 1000 mL. Standardize as in Section 5220B.3*d*.

e. Stock nitrite solution: Commercial reagent-grade $NaNO_2$ assays at less than 99%. Because NO_2^- is oxidized readily in the presence of moisture, use a fresh bottle of reagent for preparing the stock solution and keep bottles tightly stoppered against the free access of air when not in use. To determine $NaNO_2$ content, add a known excess of standard 0.01*M* (0.05*N*) $KMnO_4$ solution (see ¶ h below), discharge permanganate color with a known quantity of standard reductant such as 0.025*M* $Na_2C_2O_4$ or 0.05*M* $Fe(NH_4)_2(SO_4)_2$, and back-titrate with standard permanganate solution.

1) Preparation of stock solution—Dissolve 1.232 g $NaNO_2$ in water and dilute to 1000 mL; 1.00 mL = 250 µg N. Preserve with 1 mL $CHCl_3$.

2) Standardization of stock nitrite solution—Pipet, in order, 50.00 mL standard 0.01*M* (0.05*N*) $KMnO_4$, 5 mL conc H_2SO_4, and 50.00 mL stock NO_2^- solution into a glass-stoppered flask or bottle. Submerge pipet tip well below surface of permanganate-acid solution while

adding stock NO_2^- solution. Shake gently and warm to 70 to 80°C on a hot plate. Discharge permanganate color by adding sufficient 10-mL portions of standard 0.025*M* $Na_2C_2O_4$. Titrate excess $Na_2C_2O_4$ with 0.01*M* (0.05*N*) $KMnO_4$ to the faint pink end point. Carry a water blank through the entire procedure and make the necessary corrections in the final calculation as shown in the equation below.

If standard 0.05*M* ferrous ammonium sulfate solution is substituted for $Na_2C_2O_4$, omit heating and extend reaction period between $KMnO_4$ and Fe^{2+} to 5 min before making final $KMnO_4$ titration.

Calculate NO_2^--N content of stock solution by the following equation:

$$A = \frac{[(B \times C) - (D \times E)] \times 7}{F}$$

where:

A = mg NO_2^--N/mL in stock $NaNO_2$ solution,
B = total mL standard $KMnO_4$ used,
C = normality of standard $KMnO_4$,
D = total mL standard reductant added,
E = normality of standard reductant, and
F = mL stock $NaNO_2$ solution taken for titration.

Each 1.00 mL 0.01*M* (0.05*N*) $KMnO_4$ consumed by the $NaNO_2$ solution corresponds to 1750 µg NO_2^--N.

f. Intermediate nitrite solution: Calculate the volume, G, of stock NO_2^- solution required for the intermediate NO_2^- solution from $G = 12.5/A$. Dilute the volume G (approximately 50 mL) to 250 mL with water; 1.00 mL = 50.0 µg N. Prepare daily.

g. Standard nitrite solution: Dilute 10.00 mL intermediate NO_2^- solution to 1000 mL with water; 1.00 mL = 0.500 µg N. Prepare daily.

h. Standard potassium permanganate titrant, 0.01*M* (0.05*N*): Dissolve 1.6 g $KMnO_4$ in 1 L distilled water. Keep in a brown glass-stoppered bottle and age for at least 1 week. Carefully decant or pipet supernate without stirring up any sediment. Standardize this solution frequently by the following procedure:

Weigh to the nearest 0.1 mg several 100- to 200-mg samples of anhydrous $Na_2C_2O_4$ into 400-mL beakers. To each beaker, in turn, add 100 mL distilled water and stir to dissolve. Add 10

mL 1 + 1 H_2SO_4 and heat rapidly to 90 to 95°C. Titrate rapidly with permanganate solution to be standardized, while stirring, to a slight pink end-point color that persists for at least 1 min. Do not let temperature fall below 85°C. If necessary, warm beaker contents during titration; 100 mg will consume about 6 mL solution. Run a blank on distilled water and H_2SO_4.

$$\text{Normality of } KMnO_4 = \frac{\text{g } Na_2C_2O_4}{(A - B) \times 0.335\ 05}$$

where:

A = mL titrant for sample and
B = mL titrant for blank.

Average the results of several titrations.

4. Procedure

a. Removal of suspended solids: If sample contains suspended solids, filter through a 0.45-µm-pore-diam membrane filter.

b. Color development: If sample pH is not between 5 and 9, adjust to that range with 1*N* HCl or NH_4OH as required. To 50.0 mL sample, or to a portion diluted to 50.0 mL, add 2 mL color reagent and mix.

c. Photometric measurement: Between 10 min and 2 h after adding color reagent to samples and standards, measure absorbance at 543 nm. As a guide use the following light paths for the indicated NO_2^--N concentrations:

Light Path Length *cm*	NO_2^--N *µg/L*
1	2–25
5	2–6
10	<2

5. Calculation

Prepare a standard curve by plotting absorbance of standards against NO_2^--N concentration. Compute sample concentration directly from curve.

6. Precision and Bias

In a single laboratory using wastewater samples at concentrations of 0.04, 0.24, 0.55, and 1.04 mg $NO^-_3 + NO_2^-$-N/L, the standard deviations were ±0.005, ± 0.004, ± 0.005, and ± 0.01, respectively. In a single laboratory using wastewater samples at concentrations of 0.24, 0.55, and 1.05 mg $NO_3^- + NO_2^-$-N/L, the recoveries were 100%, 102%, and 100%, respectively.[1]

7. Reference

1. U.S. ENVIRONMENTAL PROTECTION AGENCY. 1979. Methods for Chemical Analysis of Water and Wastes. Method 353. 3. U.S. Environmental Protection Agency, Washington, D.C.

B. Whatman Guideline for the cellulose filter papers

Typical Properties - Cellulose Filters

Grade	Particle Retention* Liquid (µm)	Air Flow Rate (s/100 mL/in²)	Ash (%)	Typical Thickness (µm)	Basis Weight (g/m²)	Wet Burst (psi)	Dry Burst (psi)	Tensile M/D Dry (N/15 mm)
Qualitative								
1	11	10.5	0.06	180	88	0.3	16	39.1
2	8	21	0.06	190	103	0.7	16	44.6
3	6	26	0.06	390	187	0.5	28	72
4	20-25	3.7	0.06	205	96	0.7	10	28.4
5	2.5	94	0.06	200	98	0.4	21	55.6
6	3	35	0.2	180	105	0.3	15	39.1

contd >

Grade	Particle Retention* Liquid (µm)	Air Flow Rate (s/100 mL/in²)	Ash (%)	Typical Thickness (µm)	Basis Weight (g/m²)	Wet Burst (psi)	Dry Burst (psi)	Tensile M/D Dry (N/15 mm)
General Purpose and Wet Strengthened Qualitative								
91	10	6.2	N/A	205	71	2	18	28
93	10	7	N/A	145	67	2.6	12	38
113	30	1.3	N/A	420	131	8	24	38.6
114	23	5.3	N/A	190	77	8.9	15	42.1
Ashless Quantitative								
40	8	19.3	0.007	210	92	0.5	16	46.7
41	20-25	3.4	0.007	215	84	0.3	10	27.2
42	2.5	107	0.007	200	100	0.7	25	55.8
43	16	8.9	0.007	220	96	0.6	12	38.2
44	3	57	0.007	176	77	0.4	44	39.4
Hardened Low Ash Quantitative								
50	2.7	96	0.015	115	97	9.1	33	84
52	7	11.4	0.015	175	101	8.3	24	71.5
54	20-25	4.2	0.015	185	92	9.4	18	57.6
Hardened Ashless Quantitative								
540	8	13.2	0.006	160	88	9	20	63
541	20-25	3.8	0.006	155	82	5.3	14	43.4
542	2.7	69	0.006	150	93	9.2	28	82.6

C. Cost Analysis Calculations

	Disks diameter (cm)	Porosity (um)	Paper sheet diameter (cm)	Box Price (€)	Sheets / Box	Price/sheet (€)	Disks/sheet	Price/disk (€)	Price/layer (€)
W1	0.95	11	15	14.72	100	0.1472	164	0.0009 €	0.022 €
	1.27						98	0.0015 €	0.036 €
W50	0.95	2.7	15	48.44	100	0.4844	164	0.0030 €	0.071 €

	Price/bottle	Bottle quantity	€/g Or €/mL	Necessary quantity for preparation of 1mL reagent	Price/mL of reagent
Sulfanilamide	44.77€	100 g	0.4477 €/g	0.02 g	
N1NED	379.15€	25 g	15.166 €/g	0.002 g	0.03929€
H_3PO_4 5M	1.04€	100 mL	0.01043 €/mL	0.1 mL	

	Bottle Price	Bottle quantity (g)	€/g
Zinco	38.9 €	1000 g	0.0389 €/g

Price of box of plastic pouches	4.55 €
n.º of pouches/box	100
Price/pouch	0.046 €

D. Comparison between the developed nitrite µPAD and the colorimetric reference methods

Sample ID	Sample n.º	Ref.Met. (µM)	µPAD (µM)	%RSD
F_J_21_01	1	19.6	22.2	13.4
F_DA_21_01	2	30.5	25.4	-16.8
J_DA_21_01	3	48.5	38.2	-21.2
S_DA_21_01	4	115.3	108.8	-5.6
C_24_01	5	63.9	58.3	-8.7
T_24_01	6	72.8	65.8	-9.6
F_24_01	7	44.3	43.1	-2.7
C_DA_24_01	8	141.4	158.0	11.8
C_AA_24_01	9	49.3	44.4	-9.9
J_24_01	10	44.2	37.4	-15.5
T_28_01	11	75.6	72.6	-4.0
F_28_01	12	42.0	42.5	1.3
F_J_28_01	13	42.4	44.0	3.9
F_28_01	14	75.1	77.3	2.9
F_06_02	15	53.5	52.0	-2.7
T_06_02	16	35.4	44.5	25.9
J_06_02	17	23.1	17.7	-23.4
C_06_02	18	81.9	90.9	11.1

References

1. Word Health Organization. Standing up for the right to health [Internet]. 2018 [cited 2019 Feb 22]. Available from: https://www.who.int/news-room/feature-stories/detail/standing-up-for-the-right-to-health
2. Petti CA, Polage CR, Quinn TC, Ronald AR, Sande MA. Laboratory Medicine in Africa: A Barrier to Effective Health Care. Clin Infect Dis [Internet]. 2006 Feb 1 [cited 2018 Dec 13];42(3):377–82. Available from: https://academic.oup.com/cid/article-lookup/doi/10.1086/499363
3. McNerney R. Diagnostics for Developing Countries. Diagnostics [Internet]. 2015 [cited 2018 Dec 13];5(2):200. Available from: https://www.ncbi.nlm.nih.gov/pmc/articles/PMC4665590/
4. Jiang X, Fan ZH. Fabrication and Operation of Paper-Based Analytical Devices. Annu Rev Anal Chem [Internet]. 2016 Jun 12 [cited 2018 Dec 13];9(1):203–22. Available from: http://www.annualreviews.org/doi/10.1146/annurev-anchem-071015-041714
5. Kosack CS, Page A-L, Klatser PR. A guide to aid the selection of diagnostic tests. Bull World Health Organ [Internet]. 2017 Sep 1 [cited 2019 Feb 22];95(9):639–45. Available from: http://www.who.int/entity/bulletin/volumes/95/9/16-187468.pdf
6. Paper microfluidic devices : A review 2017 - Elveflow [Internet]. [cited 2018 Dec 13]. Available from: https://www.elveflow.com/microfluidic-tutorials/microfluidic-reviews-and-tutorials/paper-microfluidic-devices-a-review-2017/
7. Martinez AW, Phillips ST, Butte MJ, Whitesides GM. Patterned Paper as a Platform for Inexpensive, Low-Volume, Portable Bioassays. Angew Chemie [Internet]. 2007 Feb 12 [cited 2019 Feb 23];119(8):1340–2. Available from: http://doi.wiley.com/10.1002/ange.200603817
8. Almeida MIGS, Jayawardane BM, Kolev SD, McKelvie ID. Developments of microfluidic paper-based analytical devices (μPADs) for water analysis: A review. Talanta [Internet]. 2018 Jan 15 [cited 2018 Nov 20];177:176–90. Available from: https://www.sciencedirect.com/science/article/pii/S0039914017309013
9. Martinez AW, Phillips ST, Whitesides GM, Carrilho E. Diagnostics for the developing world: Microfluidic paper-based analytical devices. Anal Chem. 2010;82(1):3–10.
10. Birch NC, Stickle DF. Example of use of a desktop scanner for data acquisition in a colorimetric assay. Clin Chim Acta [Internet]. 2003 Jul 1 [cited 2018 Aug 21];333(1):95–6. Available from:

https://www.sciencedirect.com/science/article/pii/S0009898103001682?via%3Dihub

11. Ramdzan AN, Almeida MIGS, McCullough MJ, Kolev SD. Development of a microfluidic paper-based analytical device for the determination of salivary aldehydes. Anal Chim Acta. 2016;919:47–54.
12. New World Encyclopedia. Nitrite.
13. New World Encyclopedia. Nitrate [Internet]. [cited 2018 Dec 20]. Available from: http://www.newworldencyclopedia.org/entry/Nitrate
14. Lundberg JO, Weitzberg E, Cole JA, Benjamin N. Nitrate, bacteria and human health. Nat Rev Microbiol. 2004 Jul 1;2(7):593–602.
15. Moorcroft MJ, Davis J, Compton RG. Detection and determination of nitrate and nitrite: a review. Talanta [Internet]. 2001 Jun 21 [cited 2018 Jun 20];54(5):785–803. Available from: https://www.sciencedirect.com/science/article/pii/S003991400100323X
16. Atsdr. 9 NITRATE AND NITRITE 2. RELEVANCE TO PUBLIC HEALTH 2.1 BACKGROUND AND ENVIRONMENTAL EXPOSURES TO NITRATE AND NITRITE IN THE UNITED STATES [Internet]. [cited 2018 Sep 25]. Available from: https://www.atsdr.cdc.gov/toxprofiles/tp204-c2.pdf
17. VMI | NO Metabolomics Core Facility [Internet]. [cited 2018 Dec 15]. Available from: https://www.vmi.pitt.edu/NO/index.html
18. Tannenbaum SR, Sinskey AJ, Weisman M, Bishop W. Nitrite in Human Saliva. Its Possible Relationship to Nitrosamine Formation23. JNCI J Natl Cancer Inst [Internet]. 1974 Jul [cited 2018 Jun 20];53(1):75–784. Available from: https://academic.oup.com/jnci/article-lookup/doi/10.1093/jnci/53.1.79
19. Mirvish SS, Reimers KJ, Kutler B, Chen SC, Haorah J, Morris CR, et al. Nitrate and nitrite concentrations in human saliva for men and women at different ages and times of the day and their consistency over time. Eur J Cancer Prev [Internet]. 2000 Oct [cited 2018 May 13];9(5):335–42. Available from: http://www.ncbi.nlm.nih.gov/pubmed/11075887
20. Jayawardane BM, McKelvie ID, Kolev SD. Development of a gas-diffusion microfluidic paper-based analytical device (μPAD) for the determination of ammonia in wastewater samples. Anal Chem. 2015;87(9):4621–6.
21. Kerkar P. What is Blue Baby Syndrome & How is it Treated? [Internet]. 2018 [cited 2018 May 25]. Available from: https://www.epainassist.com/blood-diseases/what-is-blue-baby-syndrome-and-how-is-it-treated
22. Davis Charles. Hemoglobin Ranges: Normal, Symptoms of High and Low Levels

[Internet]. [cited 2018 Dec 15]. Available from: https://www.medicinenet.com/hemoglobin/article.htm

23. Bahadoran Z, Mirmiran P, Ghasemi A, Kabir A, Azizi F, Hadaegh F. Is dietary nitrate/nitrite exposure a risk factor for development of thyroid abnormality? A systematic review and meta-analysis. Nitric Oxide [Internet]. 2015 May 1 [cited 2018 Oct 9];47:65–76. Available from: https://www.sciencedirect.com/science/article/pii/S1089860315002049
24. Sánchez GA, Miozza VA, Delgado A, Busch L. Total salivary nitrates and nitrites in oral health and periodontal disease. Nitric Oxide [Internet]. 2014 Jan 30 [cited 2018 May 25];36:31–5. Available from: https://www.sciencedirect.com/science/article/pii/S1089860313003315?via%3Dihub
25. Doel JJ, Hector MP, Amirtham C V., Al-Anzan LA, Benjamin N, Allaker RP. Protective effect of salivary nitrate and microbial nitrate reductase activity against caries. Eur J Oral Sci [Internet]. 2004 Oct [cited 2018 Jun 20];112(5):424–8. Available from: http://doi.wiley.com/10.1111/j.1600-0722.2004.00153.x
26. Wang Q-H, Yu L-J, Liu Y, Lin L, Lu R, Zhu J, et al. Methods for the detection and determination of nitrite and nitrate: A review. Talanta [Internet]. 2017 Apr 1 [cited 2018 Oct 23];165:709–20. Available from: https://www.sciencedirect.com/science/article/pii/S0039914016309924
27. Tsikas D. Analysis of nitrite and nitrate in biological fluids by assays based on the Griess reaction: Appraisal of the Griess reaction in the l-arginine/nitric oxide area of research. J Chromatogr B Anal Technol Biomed Life Sci. 2007;851(1–2):51–70.
28. Measurement of NO2-by the Griess reaction. | Download Scientific Diagram [Internet]. [cited 2019 Feb 22]. Available from: https://www.researchgate.net/figure/Measurement-of-NO2-by-the-Griess-reaction_fig35_262499205
29. Hofman LF. Human Saliva as a Diagnostic Specimen. J Nutr [Internet]. 2001 May 1 [cited 2018 Dec 20];131(5):1621S–1625S. Available from: https://academic.oup.com/jn/article/131/5/1621S/4686814
30. Chojnowska S, Baran T, Wilińska I, Sienicka P, Cabaj-Wiater I, Knaś M. Human saliva as a diagnostic material. Adv Med Sci [Internet]. 2018 Mar 1 [cited 2018 Dec 20];63(1):185–91. Available from: https://www.sciencedirect.com/science/article/pii/S189611261730072X
31. Humphrey SP, Williamson RT. A review of saliva Normal composition, flow, and function. Humphrey, Williamson. 2001. Journal of Prosthetic Dentistry.pdf.

2001;85(2).

32. Almeida, P.D.V EA. Saliva Composition and Functions : J comtemporary Dent Pract Vol 9. 2008;9(3):72–80.
33. Tiwari M. Science behind human saliva. J Nat Sci Biol Med [Internet]. 2011 Jan [cited 2018 Dec 20];2(1):53. Available from: http://www.ncbi.nlm.nih.gov/pubmed/22470235
34. Chiappin S, Antonelli G, Gatti R, De Palo EF. Saliva specimen: A new laboratory tool for diagnostic and basic investigation. Clin Chim Acta [Internet]. 2007 Aug 1 [cited 2018 Dec 20];383(1–2):30–40. Available from: https://www.sciencedirect.com/science/article/pii/S0009898107002136
35. Saliva Collection [Internet]. [cited 2019 Jan 3]. Available from: https://www.google.com/url?sa=i&rct=j&q=&esrc=s&source=images&cd=&cad=rja&uact=8&ved=2ahUKEwiu8PnAg9LfAhVSLBoKHYNJCcIQjhx6BAgBEAM&url=https%3A%2F%2Fabwnet.org%2Fresearchers-collecting-saliva-sample.htm&psig=AOvVaw0OGnwy3QFQDb80qhd53TiC&ust=154661910679183
36. Saliva Collection (2) [Internet]. [cited 2019 Jan 3]. Available from: https://www.google.com/url?sa=i&rct=j&q=&esrc=s&source=images&cd=&cad=rja&uact=8&ved=2ahUKEwjTzu_Ng9LfAhUQyoUKHb7hD2wQjhx6BAgBEAM&url=https%3A%2F%2Fwww.youtube.com%2Fwatch%3Fv%3Dazj5b0vA2Hk&psig=AOvVaw0OGnwy3QFQDb80qhd53TiC&ust=1546619106791836%0D%0A
37. Saliva collection: gauze [Internet]. [cited 2019 Jan 3]. Available from: https://www.google.com/url?sa=i&rct=j&q=&esrc=s&source=images&cd=&cad=rja&uact=8&ved=2ahUKEwjNhb-KhNLfAhUJzhoKHWcYAy4Qjhx6BAgBEAM&url=https%3A%2F%2Fwww.transmedco.com%2Fwound-care%2FCH1806.html&psig=AOvVaw2yoorYVmviktLjvS3bWI3L&ust=1546619294808714%0D%0A
38. Saliva Collection: cotton rolls [Internet]. [cited 2019 Jan 3]. Available from: https://www.google.com/url?sa=i&rct=j&q=&esrc=s&source=images&cd=&cad=rja&uact=8&ved=2ahUKEwi63Ny0hNLfAhUQaBoKHd5-BRwQjhx6BAgBEAM&url=https%3A%2F%2Fdir.indiamart.com%2Fimpcat%2Fcotton-dental-roll.html&psig=AOvVaw0ORHxmYXocyKwfyfUEuw7f&ust=1546619379379930
39. Eisenbrand G, Spiegelhalder B, Preussmann R. Nitrate and nitrite in saliva. Oncology [Internet]. 1980 [cited 2018 May 26];37(4):227–31. Available from:

http://www.ncbi.nlm.nih.gov/pubmed/7443155

40. Teixeira CFCP, Segundo RLA, Rangel AOSS, Mesquita RBR, Ferreira MTSOB, Bordalo AA. Development of a sequential injection system for the determination of nitrite and nitrate in waters with different salinity: Application to estuaries in NW Portugal. Anal Methods. 2009;1(3):195.
41. Wikipedia. Complementary Colors.
42. Jayawardane BM, Wei S, McKelvie ID, Kolev SD. Microfluidic Paper-Based Analytical Device for the Determination of Nitrite and Nitrate. Anal Chem [Internet]. 2014 Aug 5 [cited 2018 Jun 20];86(15):7274–9. Available from: http://pubs.acs.org/doi/10.1021/ac5013249
43. Wiegand A, Batista GR, Torres CRG, Sener B, Attin T. Artificial Saliva Formulations versus Human Saliva Pretreatment in Dental Erosion Experiments. Caries Res. 2016;50(1):78–86.
44. Currie LA. Nomenclature in evaluation of analytical methods including detection and quantification capabilities (IUPAC Recommendations 1995). Pure Appl Chem [Internet]. 1995 Jan 1 [cited 2019 Feb 24];67(10):1699–723. Available from: http://www.degruyter.com/view/j/pac.1995.67.issue-10/pac199567101699/pac199567101699.xml